Available online at www.sciencedirect.com
ScienceDirect
Journal of Sound and Vibration 303 (2007) 475–500
JOURNAL OF SOUND AND VIBRATION
www.elsevier.com/locate/jsvi

Viscous damping identification in linear vibration

A. Srikantha Phani, J. Woodhouse*

Department of Engineering, University of Cambridge, Trumpington Street, Cambridge CB2 1PZ, UK

Received 28 September 2005; received in revised form 4 December 2006; accepted 19 December 2006

Abstract

Parametric identification of viscous damping models in the context of linear vibration theory is studied. Frequency domain identification methods based on measured frequency response functions (FRFs) are considered. Existing methods are classified into two main groups: matrix methods which use directly the measured FRF matrix, and modal methods which use modal parameters deduced from the FRFs. A new group of methods called enhanced methods is introduced to improve the performance of the matrix methods. These three groups of identification methods are critically reviewed and a systematic simulation study is then conducted to compare their performance. Four simulation examples are presented to bring out the relative merits of the identification methods. The success of each method is evaluated with reference to four norms introduced. Robust methods of identification are identified.

1. Introduction

All vibrating systems exhibit damping, yet the modelling and identification of physical mechanisms of damping is very rudimentary in the current state of the art. For a comprehensive review on damping in structural vibrations see Refs. [1–4]. While there are well-developed methods, such as the finite element (FE) method [5], to model the inertial (mass) and elastic (stiffness) properties of engineering structures, damping modelling tends to be based on ad hoc assumptions, chosen more for mathematical convenience than physical accuracy. There are numerous individual mechanisms which collectively manifest as damping, and this complexity of detail is the main obstacle to the development of a comprehensive theory of damping. A typical built-up structure, such as an aircraft fuselage, can lose energy through viscoelastic effects within the material (material damping), through phenomena such as friction or air-pumping which occur at interfaces and joints, or through the contact with the fluid in which the structure vibrates. Examined in detail most of these mechanisms are nonlinear. However, linear damping models often suffice for small oscillations and small damping. Given the variety and complexity of damping mechanisms, much of the modelling effort has been restricted to viscous damping.

Several methods have been proposed in the literature to identify the parameters of a viscous damping matrix from measurements on a vibrating system. Although each identification method has been validated by one-off

*Corresponding author. Fax: +44 1223 332662.
E-mail address: jw12@cam.ac.uk (J. Woodhouse).

0022-460X/$ - see front matter
doi:10.1016/j.jsv.2006.12.031

simulations, the literature contains no systematic study aimed at comparing their relative merits and drawbacks. It is very difficult, given the abundance of algorithms, to judge their realistic performance.

This paper has three objectives. The first is to collect different identification methods described in the literature and classify them in order to compare their merits and deficiencies. The second objective is to propose new approaches to damping identification to overcome the limitations of the existing ones. Finally, the methods are compared for their performance on selected simulation case studies. All methods considered in the present study are restricted to the frequency domain, i.e. methods which are based on frequency response functions (FRFs) or deduced modal parameters. Only viscous damping models are considered; non-viscous models are addressed elsewhere [6], since space does not permit a full treatment of non-viscous models here. The intention of this paper is to give a systematic survey of all relevant methods and compare them with the new methods to be proposed. This inevitably means that the list of methods to be considered is quite long. It is felt that to reduce the list would not give a full and fair representation.

For convenience of discussion, a choice has been made to classify damping identification methods in the frequency domain into three major groups:

(1) Matrix methods; based directly on the FRF matrix.
(2) Modal methods; based on modal parameters deduced from the FRFs.
(3) Enhanced methods; variants of the matrix methods to improve accuracy or reduce the number of measurements needed.

Modal-based methods use complex modeshapes and natural frequencies identified from modal testing [7,8], in some cases together with knowledge of the mass and/or stiffness matrices obtained from analytical means such as the FE method. Matrix methods use the full FRF matrix to obtain the mass, stiffness and damping matrices. They do not require an FE model a priori. Enhanced methods are possible improvements of matrix methods proposed in this study, designed to overcome limitations of the previous methods by combining beneficial features of the modal and the matrix methods. A list of damping identification methods drawn from the literature together with some new algorithms which will be presented in this paper is given below:

(1) Matrix methods
  (a) Lee and Kim's method [9].
  (b) Chen, Ju and Tseui's method [10].
  (c) Instrumental variable method [11].
  (d) Matrix perturbation method, a new method proposed in this paper.
(2) Modal methods
  (a) Adhikari's methods to identify viscous and symmetrised viscous damping matrices [12,13].
  (b) Lancaster's method [14].
  (c) Minas and Inman's method [15].
  (d) Ibrahim's method [16].
(3) Enhanced methods
  (a) Matrix methods using expanded FRFs.
  (b) Matrix methods using reconstructed FRFs.
  (c) Matrix methods using SVD-approximated FRFs.

A brief review of the above algorithms is presented in Sections 2–4. A detailed study comparing the performance of each method is presented in Sections 5–11.

2. Matrix methods

The dynamic response of a continuous structure, such as a beam or a plate, in any given frequency range containing a finite number of modes, can always be approximated by a discrete spring–mass–dashpot system. These discrete systems which are approximations to a continuous system over a frequency range will be referred to as multi degree of freedom (mdof) systems and they are governed by ordinary differential equations of motion given as follows for systems with viscous damping:

$$\mathbf{M}\ddot{\mathbf{x}} + \mathbf{C}\dot{\mathbf{x}} + \mathbf{K}\mathbf{x} = \mathbf{f}. \tag{1}$$

In the above equation $\mathbf{M}$, $\mathbf{K}$ and $\mathbf{C}$ are, respectively, the mass, stiffness and viscous damping matrices; $\mathbf{x}$ and $\mathbf{f}$, respectively, denote the response and generalised force corresponding to each dof. These equations of motion can be re-written in the frequency domain as

$$[-\omega^2\mathbf{M} + \mathrm{i}\omega\mathbf{C} + \mathbf{K}]\mathbf{X}(\omega) = \mathbf{F}(\omega), \tag{2}$$

where $\mathbf{X}(\omega)$ and $\mathbf{F}(\omega)$ are, respectively, the Fourier transform of the response $\mathbf{x}$ and force $\mathbf{f}$. From Eq. (2) two matrices may be defined: the FRF matrix $\mathbf{H}$, and its inverse the dynamic stiffness matrix $\mathbf{D}$:

$$\mathbf{H}(\omega) \equiv [-\omega^2\mathbf{M} + \mathrm{i}\omega\mathbf{C} + \mathbf{K}]^{-1}, \quad \mathbf{D}(\omega) \equiv \mathbf{H}^{-1} = [-\omega^2\mathbf{M} + \mathrm{i}\omega\mathbf{C} + \mathbf{K}]. \tag{3}$$

In experiments the FRF matrix $\mathbf{H}(\omega)$ is measured: the objective is to use it to find the viscous damping matrix $\mathbf{C}$. The above relationships in the frequency domain serve as a starting point for the identification procedure for matrix methods. Note that if the system has non-viscous but still linear damping mechanisms then the constant matrix $\mathbf{C}$ is replaced by a frequency dependent matrix $\mathscr{G}(\omega)$ [17]. Such non-viscous damping models and their identification are not within the scope of the present work.

Two approaches can be taken to identify a viscous damping matrix from the measured FRF matrix. The first approach is to invert the FRF matrix to obtain the dynamic stiffness matrix and then obtain the damping matrix. Typical examples of this approach are the identification methods proposed by Lee and Kim [9] and Chen et al. [10]. An iterative variant of this approach is the instrumental variable method [11]. The second approach is based on the small damping assumption and uses a perturbation expansion for the matrix inverse. This method is based on the measurement of the full FRF matrix and hence is classified under matrix methods here even though it also uses modal parameters.

2.1. Lee and Kim's method

The method proposed by Lee and Kim [9] relies on the dynamic stiffness matrix obtained by inverting the FRF matrix. The real and imaginary parts of the dynamic stiffness matrix are:

$$\mathrm{Re}(\mathbf{D}(\omega)) = \mathbf{K} - \omega^2\mathbf{M} \quad \text{and} \quad \mathrm{Im}(\mathbf{D}(\omega)) = \omega\mathbf{C}. \tag{4}$$

These equations can be rewritten as

$$[\mathbf{I} \quad -\omega^2\mathbf{I}]\begin{bmatrix}\mathbf{K}\\ \mathbf{M}\end{bmatrix} = \mathrm{Re}(\mathbf{D}(\omega)) \tag{5}$$

and

$$\omega\mathbf{C} = \mathrm{Im}(\mathbf{D}(\omega)). \tag{6}$$

Note that the above equations are defined at a single frequency point. Assuming that $\mathbf{K}$, $\mathbf{M}$ and $\mathbf{C}$ are constant, the data from a minimum of two points is sufficient for the identification of all three matrices. In practice this is optimistic due to measurement noise, and a least squares solution is needed. The choice of frequency influences the accuracy: the FRF measurements are most accurate around each resonance peak and hence these data points are recommended. The data corresponding to anti-resonances is not accurate and hence will reduce the accuracy of the identification method. For a detailed discussion of the influence on damping identification of different experimental sources of errors, such as noise, instrumentation delays and residuals see Ref. [6].

2.2. Chen, Ju and Tseui's method

The previous method tries to identify all the three matrices, namely, the mass, stiffness and damping matrices *simultaneously*. Since the order of magnitude of the elements of the damping matrix is typically smaller than that of the stiffness or mass coefficients, the identified damping matrix may tend to have large error relative to that of the stiffness or mass matrix coefficients. The accuracy of the identified damping matrix might be improved if the identification of the damping matrix is separated from that of the mass and stiffness matrices. This is the key motivation behind the method proposed by Chen et al. [10].

Chen et al. define the "normal" frequency response function $\mathbf{H}^N(\omega)$ as

$$\mathbf{H}^N(\omega) \equiv [\mathbf{K} - \omega^2\mathbf{M}]^{-1}. \tag{7}$$

With the above definition, Eq. (2) can be written in terms of the normal frequency response as

$$[\mathbf{H}^N(\omega)]^{-1}\mathbf{X}(\omega) + \mathrm{i}\omega\mathbf{C}\mathbf{X}(\omega) = \mathbf{F}(\omega) \quad \text{or} \quad \mathbf{X}(\omega) + \mathrm{i}\mathbf{G}(\omega)\mathbf{X}(\omega) = \mathbf{H}^N(\omega)\mathbf{F}(\omega), \tag{8}$$

where $\mathbf{G}(\omega)$, referred to as the transformation matrix, is given by

$$\mathbf{G}(\omega) = \omega\mathbf{H}^N(\omega)\mathbf{C}. \tag{9}$$

Using Eq. (8) and recalling that the FRF matrix, by definition, satisfies the relation $\mathbf{X}(\omega) = \mathbf{H}(\omega)\mathbf{F}(\omega)$, one obtains the relation between the "normal" FRF matrix and the measured FRF matrix:

$$\mathbf{H}^N(\omega) = [\mathbf{I} + \mathrm{i}\mathbf{G}(\omega)]\mathbf{H}(\omega), \tag{10}$$

where $\mathbf{I}$ is an identity matrix. Noting that $\mathbf{H}^N(\omega)$ and $\mathbf{G}(\omega)$ are real matrices and hence setting the imaginary part of the RHS in Eq. (10) to zero gives

$$\mathbf{G}(\omega) = -\mathrm{Im}(\mathbf{H}(\omega))[\mathrm{Re}(\mathbf{H}(\omega))]^{-1}. \tag{11}$$

Using Eqs. (11) and (9), the damping matrix at any given frequency ω is given by

$$\mathbf{C} = \frac{1}{\omega}[\mathbf{H}^N(\omega)]^{-1}\mathbf{G}. \tag{12}$$

The above equation can be solved in a least squares sense over several frequency points to reduce the effect of measurement noise. Furthermore, symmetry of the damping matrix can be imposed to reduce the number of unknowns from N^2 elements to $N(N+1)/2$ upper or lower-triangular elements of the matrix.

2.3. *Instrumental variable method*

This technique was developed for parameter estimation problems arising in the area of econometrics. Later it was applied to structural dynamics by Fritzen [11]. Since the dynamic stiffness matrix $\mathbf{D}$ is the inverse of the FRF matrix $\mathbf{H}$, the error to be minimised in order to estimate the system matrices by a least squares procedures is given by

$$\mathbf{E} = \mathbf{H}(\omega)\mathbf{D}(\omega) - \mathbf{I}, \tag{13}$$

where $\mathbf{I}$ is the identity matrix and $\mathbf{E}$ is the error matrix. By separating the real and imaginary parts and using Eq. (3), the above equations can be written as

$$\begin{bmatrix} \mathrm{Re}(-\omega^2\mathbf{H} & \mathrm{i}\omega\mathbf{H} & \mathbf{H}) \\ \mathrm{Im}(-\omega^2\mathbf{H} & \mathrm{i}\omega\mathbf{H} & \mathbf{H}) \end{bmatrix} \begin{bmatrix} \mathbf{M} \\ \mathbf{C} \\ \mathbf{K} \end{bmatrix} = \begin{bmatrix} \mathbf{I} \\ \mathbf{0} \end{bmatrix} + \begin{bmatrix} \mathrm{Re}(\mathbf{E}) \\ \mathrm{Im}(\mathbf{E}) \end{bmatrix}. \tag{14}$$

The instrumental variable method proposes an *iterative* solution of the form:

$$[\mathbf{M}\ \ \mathbf{C}\ \ \mathbf{K}]^{\mathrm{T}}_{m+1} = [\mathbf{W}^{\mathrm{T}}_m\mathbf{A}]^{-1}\mathbf{W}^{\mathrm{T}}_m\bar{\mathbf{I}}, \tag{15}$$

where $\mathbf{W}$ is the so called "instrumental variable" to be chosen by the user. The matrices $\mathbf{A}$ and $\bar{\mathbf{I}}$ are defined as

$$\mathbf{A} \equiv [\mathbf{A}_1 \ldots \mathbf{A}_k \ldots \mathbf{A}_N]^{\mathrm{T}}, \quad \mathbf{A}_k \equiv \begin{bmatrix} \mathrm{Re}(-\omega_k^2\mathbf{H} & \mathrm{i}\omega_k\mathbf{H} & \mathbf{H}) \\ \mathrm{Im}(-\omega_k^2\mathbf{H} & \mathrm{i}\omega_k\mathbf{H} & \mathbf{H}) \end{bmatrix}, \quad \bar{\mathbf{I}} \equiv \left[\begin{bmatrix} \mathbf{I} \\ \mathbf{0} \end{bmatrix} \cdots \begin{bmatrix} \mathbf{I} \\ \mathbf{0} \end{bmatrix}\right]^{\mathrm{T}}. \tag{16}$$

The choice of the matrix $\mathbf{W}$ is an important issue. For the present problem it is chosen as the "analytical" dynamic stiffness matrix which can be obtained at each stage of iteration from the identified system matrices in the previous iteration: $\mathbf{W}_{m+1} = [-\omega^2\mathbf{M}_m + \mathrm{i}\omega\mathbf{C}_m + \mathbf{K}_m]^{-1}$. The matrices with subscript m are those identified in the mth stage of iteration. The linear least squares solution obtained using the real and imaginary parts of the "measured" dynamic stiffness (the inverse of the raw measurements) provides the initial guess to start the iteration procedure. The convergence can be checked by various criteria which can be based on:

- The convergence of the norm of each of the system matrices.
- Convergence of the natural frequencies obtained by solving the eigenvalue problem of the undamped system.
- Minimisation of the difference between the measured FRF matrix $\mathbf{H}$ and the reconstructed FRF $\mathbf{H}_{rm}$ obtained by $\mathbf{H}_{rm} = [\mathbf{K}_m - \omega^2\mathbf{M}_m + \mathrm{i}\omega\mathbf{C}_m]^{-1}$, at the mth iteration.

This method gives the converged mass, stiffness and damping matrices with respect to a predefined convergence criterion. Significant computational effort is required for large matrices. This method can be considered as an iterative variant of Lee and Kim's method. However, as will be shown later, its performance is not the same as that of Lee and Kim's method.

2.4. Matrix perturbation method

A new method which relies on the FRF matrix and the modal parameters is proposed in this section. This method combines the results from first-order perturbation theory for complex modes [17,18] with a series expansion [19,20] for the FRF matrix of a viscously damped system. It has the advantage of separating the damping identification from that of the mass and stiffness matrices.

The identification is performed in two stages. In the first stage, the diagonal part of the modal damping matrix is obtained from the modal parameters deduced from the FRFs. In the second stage the off-diagonal terms of the modal damping matrix are obtained using a perturbation expansion. Firstly, the expression for FRF in Eq. (3) can be written as

$$\mathbf{H}'(\omega) = [-\omega^2\mathbf{I} + \mathrm{i}\omega\mathbf{C}' + \mathbf{\Lambda}]^{-1}, \tag{17}$$

where $\mathbf{C}'$ is the damping matrix in modal coordinates, $\mathbf{\Lambda}$ is a diagonal matrix with squared undamped natural frequencies as its diagonal entries and $\mathbf{I}$ is the identity matrix. In experiments the modal damping factors determine the diagonal part ($\mathbf{C}'_d$). To identify the off-diagonal terms ($\mathbf{C}'_o$), a standard series expansion for the inverse of a sum of matrices [21] is used. Such an expansion has been used by Bhaskar [19,20] in the context of studying the errors due to approximating non-classically damped systems by proportional viscous damping. Woodhouse has also used similar perturbation analysis in Ref. [17]. Define $\mathbf{A}(\omega) \equiv \mathbf{\Lambda} - \omega^2\mathbf{I} + \mathrm{i}\omega\mathbf{C}'_d$. The FRF expression in Eq. (17) can be approximated up to the leading order term in $\mathbf{C}'_o$ as

$$\mathbf{H}(\omega) = [\mathbf{A}(\omega) + \mathrm{i}\omega\mathbf{C}'_o]^{-1} \approx \mathbf{A}^{-1}(\omega) - \mathrm{i}\omega\mathbf{A}^{-1}(\omega)\mathbf{C}'_o\mathbf{A}^{-1}(\omega). \tag{18}$$

The procedure for damping identification is thus:

(1) Measure the full FRF matrix $\mathbf{H}(\omega)$ on the test structure with a suitable choice of grid points.
(2) Identify the real modes $\mathbf{U}$, damping factors (Q factors) and natural frequencies for each mode using modal identification procedures.
(3) The diagonal terms of the damping matrix in modal coordinates are given by $\mathbf{C}'_{d_{nn}} = \omega_n/Q_n$, where ω_n and Q_n are, respectively, the natural frequency and Q factor of the nth mode.
(4) The off-diagonal terms of the damping matrix in modal coordinates are given by

$$\mathbf{C}'_o \approx \frac{\mathbf{A}(\omega) - \mathbf{A}(\omega)\mathbf{H}(\omega)\mathbf{A}(\omega)}{\mathrm{i}\omega}. \tag{19}$$

(5) Obtain the full modal damping matrix $\mathbf{C}' = \mathbf{C}'_d + \mathbf{C}'_o$.
(6) Transform back to physical coordinates $\mathbf{C} = [\mathbf{U}^T]^{-1}\mathbf{C}'\mathbf{U}$.

The above procedure yields a frequency dependent damping matrix **C** when repeated at each frequency point. A least squares solution can be obtained by considering a range of frequency points.

3. Methods based on modal parameters

3.1. Adhikari's methods

It is well known to experimentalists that the modeshapes found during vibration testing or modal parameter estimation procedures in general turn out to be complex. The possible usefulness of such complex modes in identifying linear damping models, both viscous and non-viscous, has been explored by Adhikari and Woodhouse [12,13,17,22]. It was shown in their study that with accurate complex modes one can identify, in principle, the parameters of viscous and certain non-viscous damping models, and also the detailed spatial distribution of damping sources within a vibrating system. Only viscous damping identification methods are considered here.

The procedure to identify the viscous damping matrix from complex modes, proposed in Ref. [22], is as follows:

(1) Measure a set of frequency response functions $\mathbf{H}_{ij}(\omega)$.
(2) Choose the number of modes (m) to be retained in the study. Determine the complex natural frequencies $\overline{\omega}_j = \omega_j(1 + (\mathrm{i}/2Q_j))$ and complex modes $\boldsymbol{\psi}_j$ from the frequency response functions, for all $j = 1, \ldots, m$, and form the complex modeshape matrix $\boldsymbol{\Psi} = [\boldsymbol{\psi}_1 \boldsymbol{\psi}_2 \ldots \boldsymbol{\psi}_m]$.
(3) Estimate the undamped natural frequencies $\omega_j = \mathrm{Re}(\overline{\omega}_j)$.
(4) Set $\mathbf{U} = \mathrm{Re}(\boldsymbol{\Psi})$ and $\mathbf{V} = \mathrm{Im}(\boldsymbol{\Psi})$, from these obtain $\mathbf{W} = \mathbf{U}^{\mathrm{T}}\mathbf{V}$ and $\mathbf{D} = \mathbf{U}^{\mathrm{T}}\mathbf{U}$.
(5) From the matrix $\mathbf{B}$ get $C'_{jk} = (\omega_j^2 - \omega_k^2)B_{kj}/\omega_j$ for $k \neq j$ and $C'_{jj} = 2\,\mathrm{Im}(\overline{\omega}_j)$.
(6) Transform the identified modal damping matrix to physical coordinates using $\mathbf{C} = [\mathbf{W}^{-1}\mathbf{U}^{\mathrm{T}}]^{\mathrm{T}}\mathbf{C}'[\mathbf{W}^{-1}\mathbf{U}^{\mathrm{T}}]$.

The viscous damping matrix identified using the above procedure need not always be symmetric. This anomalous behaviour of the viscous damping identification is rectified by a symmetry-preserving method proposed by the same authors [12], the details of which need not be discussed here.

3.2. Lancaster's method

Lancaster [14] has proposed simple results to identify the mass, stiffness and damping matrices simultaneously from the measured complex modal parameters when the complex modes are normalised in a specified way. The eigenvalue problem associated with viscously damped systems is first written in the form

$$[\lambda_j^2\mathbf{M} + \lambda_j\mathbf{C} + \mathbf{K}]\boldsymbol{\psi}_j = 0, \tag{20}$$

where **M**, **K** and **C** are, respectively, the mass, stiffness and viscous damping matrices, and $\boldsymbol{\psi}_j$ is the eigenvector (complex in general) corresponding to the eigenvalue $\lambda_j = \mathrm{i}\omega_j$. Based on the eigenvalue problem Eq. (20), Lancaster [14] has given explicit formulae for the computation of mass, stiffness and damping matrices:

$$\begin{aligned}
&\mathbf{M} = [\boldsymbol{\Psi}\boldsymbol{\Lambda}\boldsymbol{\Psi}^{\mathrm{T}} + \overline{\boldsymbol{\Psi}}\,\overline{\boldsymbol{\Lambda}}\boldsymbol{\Psi}^{H}]^{-1}\\
&\mathbf{K} = -[\boldsymbol{\Psi}\boldsymbol{\Lambda}^{-1}\boldsymbol{\Psi}^{\mathrm{T}} + \overline{\boldsymbol{\Psi}}\,\overline{\boldsymbol{\Lambda}}^{-1}\boldsymbol{\Psi}^{H}]^{-1}\\
&\mathbf{C} = -\mathbf{M}[\boldsymbol{\Psi}\boldsymbol{\Lambda}^{2}\boldsymbol{\Psi}^{\mathrm{T}} + \overline{\boldsymbol{\Psi}}\,\overline{\boldsymbol{\Lambda}}^{2}\boldsymbol{\Psi}^{H}]\mathbf{M}, \text{ where}\\
&\boldsymbol{\Lambda} = \mathrm{diag}(\lambda_j), \quad \boldsymbol{\Psi} = [\boldsymbol{\psi}_j], \quad j = 1 \ldots N
\end{aligned} \tag{21}$$

provided the eigenvector $\boldsymbol{\psi}_j$ is normalised according to

$$\boldsymbol{\psi}_j^{\mathrm{T}}[2\lambda_j\mathbf{M} + \mathbf{C}]\boldsymbol{\psi}_j = 1. \tag{22}$$

In the above equations the superscripts T, −, H, respectively denote the transpose, complex conjugate and Hermitian transpose of the matrix. The snag with this approach is that the normalisation condition in Eq. (22) requires the very knowledge of the mass and damping matrices whose identification is the objective of the method. Although the mass matrix can be obtained independently by methods such as the FE method, the damping matrix cannot be obtained analytically. To circumvent this problem, Pilkey has proposed an iterative method [23].

This iterative procedure assumes that the mass matrix is known, in addition to the identified complex modal parameters. The iteration procedure is as follows:

(1) Make an initial guess for the damping matrix, say the damping matrix with only diagonal terms of the modal damping matrix.
(2) Normalise the modeshapes such that the normalisation condition given by Eq. (22) is satisfied. This gives a new $\mathbf{\Psi}$.
(3) With the new complex modes, obtain the new damping matrix using Eq. (21).
(4) Repeat steps 2 and 3 till the damping matrix converges.

3.3. Minas and Inman's method

Minas and Inman [15] have proposed a method for identifying the damping matrix of a structure from experimental data combined with a reasonable representation of the mass and stiffness matrices developed by finite element methods and reduced by standard model reduction techniques. In this method, the eigenvalue problem in Eq. (20) is rearranged to give:

$$\mathbf{C}\boldsymbol{\psi}_j = -\frac{1}{\lambda_j}[\lambda_j^2\mathbf{M} + \mathbf{K}]\boldsymbol{\psi}_j. \tag{23}$$

Noting that $\mathbf{C}$ is real and symmetric, the complex conjugate transpose of Eq. (23) is:

$$\boldsymbol{\psi}_j^H\mathbf{C} = \mathbf{f}_j^H, \quad \mathbf{f}_j = -\frac{1}{\lambda_j}[\lambda_j^2\mathbf{M} + \mathbf{K}]\boldsymbol{\psi}_j. \tag{24}$$

In this method, the complex modes $\boldsymbol{\psi}_j$ are identified from experiments using modal parameter estimation techniques. Having identified these parameters, it is possible to identify the damping matrix using Eq. (24). The original implementation of this algorithm made use of the symmetry of the damping matrix and separating Eq. (24) into real and imaginary parts. As a consequence of the assumed symmetry of the damping matrix, the number of unknowns in the $N \times N$ damping matrix can be reduced to $N(N+1)/2$. Eq. (24) can be rearranged to form a set of linear algebraic equations in these unknowns, which can be solved directly.

3.4. Ibrahim's method

Ibrahim's method [16] requires that an analytical, finite element (FE), model of the structure is known a priori in addition to the measured modal (complex) parameters. The complex modal parameters $\boldsymbol{\psi}_i$ and λ_i, $i = 1\ldots m$, associated with the m modes, at n measurement points on the test structure ($n \geqslant m$) are obtained from a modal test. The analytical model consists of the mass matrix $\mathbf{M}$ in physical coordinates and the stiffness matrix $\mathbf{K}$. Normal modes $\boldsymbol{\phi}_i$, $i = 1\ldots n$ and natural frequencies ω_i are computed using the analytical model by solving the eigenvalue problem:

$$\mathbf{K}\boldsymbol{\phi}_j = \omega_j^2\mathbf{M}\boldsymbol{\phi}_j. \tag{25}$$

The identification of the damping matrix involves three stages:

(1) Identifying the matrices $\mathbf{A} = \mathbf{M}^{-1}\mathbf{K}$ and $\mathbf{B} = \mathbf{M}^{-1}\mathbf{C}$ from the eigenvalue problem of the damped system in Eq. (20) using the measured modal test data.

(2) Converting the measured complex modes to real modes in order to obtain a corrected mass matrix.
(3) Computation of the corrected mass matrix and hence the damping matrix using the above identified **B** matrix.

The implementation details of this method can be obtained from Refs. [6,16].

4. Enhanced methods

In the previous sections, different identification methods based on modal parameters and the FRF matrix have been considered. It is useful to consider briefly the relative merits and drawbacks of these two groups of methods. Modal methods require relatively straightforward measurements: usually only one row or column of the FRF matrix would be measured since this gives sufficient information for modal parameter extraction. However, these methods are susceptible to errors in modal parameter estimation, and accurate identification of complex modes in particular. Matrix methods have several advantages over methods which rely on modal parameters: closely spaced modes which are difficult to identify by modal fitting techniques no longer pose a problem to matrix methods, and the identified mass, stiffness and damping matrices can be directly compared with FE models without having to perform any modal analysis. However, these methods require substantial experimental effort in that one needs to measure the FRF for each input and output dof. This may result in excessive testing of the structure. Thus it is of interest to explore methods which can make matrix methods more accurate and easier to implement.

Three such enhanced methods are described in this section. The advantage of these methods when applied to matrix methods is to reduce the number of measurements and/or decrease their susceptibility to noise. Enhanced methods do not influence the performance of the modal methods.

4.1. Expansion of FRFs

The objective of this method is to reduce the number of measurements and the effect of measurement noise on the damping identification methods. Expansion of FRFs is a technique that can considerably reduce the number of measurements. The modal properties of the structure are established first from a single-reference modal test. Once the modal parameters are established, the full FRF *matrix* is given by [17]

$$\mathbf{H}(\omega) = \sum_n \left[\frac{a_n \boldsymbol{\psi}_n \boldsymbol{\psi}_n^{\mathrm{T}}}{\mathrm{i}\omega - \lambda_n} + \frac{\overline{a}_n \overline{\boldsymbol{\psi}}_n \boldsymbol{\psi}_n^{H}}{\mathrm{i}\omega - \overline{\lambda}_n} \right] \quad \text{where } a_n = \frac{1}{\boldsymbol{\psi}_n^{\mathrm{T}}[2\lambda_n \mathbf{M} + \mathbf{C}]\boldsymbol{\psi}_n}. \tag{26}$$

It can be noted from the above equation that the residue matrix for any mode, say n, is a dyadic product of the corresponding modeshape vector, i.e. $\mathbf{R}_n = a_n \boldsymbol{\psi}_n \boldsymbol{\psi}_n^{\mathrm{T}}$. The scaling factor a_n can be chosen to satisfy the unit modal mass normalisation condition. Thus the entire FRF matrix can be synthesised by using the modal parameters, i.e. complex modeshapes ($\boldsymbol{\psi}$) and complex natural frequencies (λ). The modal parameters can be obtained by applying modal fitting techniques, such as the circle fitting method or rational fraction polynomial method [7,8], to one row or column of the FRF matrix. The degenerate case of repeated modes and modes difficult to isolate by a single reference test may require additional reference tests in practice. Nevertheless it is possible in principle to synthesise the full FRF matrix from the modal parameters obtained from just one row or column of the FRF matrix.

4.2. FRF reconstruction

This method is based on the observation that the reconstructed FRFs synthesised using the modal parameters are less noisy than the raw measurements. Modal parameter estimation methods can be used to reconstruct the measured FRFs. Provided that the modal parameters have been accurately identified, the reconstructed FRFs are a good approximation to actual measurement and hence can be used to identify the damping matrix. The principal advantage of this method is noise reduction. There is no reduction in the number of measurements required, i.e. the full FRF matrix needs to be measured.

4.3. SVD analysis of FRFs

Yet another means of reducing the effect of measurement noise is provided by the singular value decomposition (SVD) technique. It is a widely used numerical technique to express any $M \times N$ matrix $\mathbf{A}$ ($M \geqslant N$) as a product of an $M \times N$ column-orthogonal matrix $\mathbf{U}$, $N \times N$ diagonal matrix $\mathbf{W}$ with positive or zero elements, and the transpose of an $N \times N$ row-orthogonal matrix $\mathbf{V}$ [24]. Thus the SVD of the FRF matrix $\mathbf{H}(\omega)$ at any given frequency ω is given by

$$\mathbf{H}(\omega) = \mathbf{U}\mathbf{W}\mathbf{V}^{\mathrm{T}}. \tag{27}$$

The diagonal matrix $\mathbf{W}$ is given by $\mathbf{W} = \mathrm{diag}[\sigma_1, \sigma_2, \ldots, \sigma_N]$, where σ_1, etc. are singular values. The singular values of the FRF matrix at any given frequency are a measure of the contribution of various modes to the frequency response. Singular values of larger magnitudes contribute more towards the response than smaller singular values. In the presence of small noise, i.e. good signal to noise ratio, the smaller singular values are more contaminated (due to their low energy content) than the larger singular values. By truncating the singular values of smaller magnitude and corresponding singular vectors we reduce the effect of noise on the measured FRFs.

A key step in the above procedure is to choose the threshold below which the singular values are truncated. If the noise matrix $\mathbf{E}$ added to the FRF matrix $\mathbf{H}$ is known a priori as is the case in simulations, then singular value rejection criteria can be based on perturbation results. It is well known that when the matrix $\mathbf{H}$ is perturbed by a noise matrix $\mathbf{E}$ then the singular values of $\mathbf{H}$ are perturbed by at most $\varepsilon = \|\mathbf{E}\|$ where $\|(\cdot)\|$ is a Euclidean norm [21]. Thus, one can ignore the singular values less than ε. The choice of threshold to truncate singular values for noise removal is an active and current area of research [25]. Note that the truncation of singular values is performed at each frequency. This is motivated by the physical observation that at any frequency only a few modes of the system govern the response; the contribution of other modes is negligible and subsumed by the noise inherent in the measurement. The FRF matrix was reconstructed using Eq. (27) by successively increasing the number of singular values retained till a convergence of the Euclidean norm of the SVD-reconsctructed FRF in Eq. (27) was obtained.

5. Comparison of performance

A wide range of damping identification methods in the frequency domain has been presented. The question is now addressed of how well they perform on a range of simple but carefully chosen systems. These simulations explore various aspects of a typical measurement scenario: noise in the measured FRFs; modal overlap and its influence on modal identification errors; modal and spatial truncation errors. A number of interesting questions can be asked:

(1) Given vibration measurements from a test structure, what is (are) the best method(s) of damping identification?
(2) What is the sensitivity of damping identification methods to errors such as noise and truncation?
(3) Do enhanced methods improve the performance of matrix methods?
(4) What is the influence of modal/spatial incompleteness on damping identification?
(5) Does accurate fitting of FRFs ensure that the underlying damping mechanisms/spatial distribution of damping are well fitted?

First it is necessary to formulate measures of performance against which the success or otherwise of each identification method can be judged. The following features need to be taken into consideration while devising suitable measures of performance:

(1) numerical accuracy of the identified damping matrix;
(2) accuracy of the modal damping factors predicted by the identified damping matrix;
(3) accuracy of the spatial distribution of damping of the identified damping matrix;
(4) accuracy of reconstructed FRFs synthesised using the identified damping matrix.

These naturally lead to four performance measures. To quantify the numerical accuracy of the identified damping matrix it is natural to introduce the *absolute norm* defined as

$$N_{\text{abs}} \equiv \left| \frac{\|\mathbf{C}_f - \mathbf{C}\|}{\|\mathbf{C}\|} \right|, \tag{28}$$

where $\mathbf{C}_f$ and $\mathbf{C}$ are, respectively, the fitted damping matrix and the actual damping matrix used in simulation, $\|(\bullet)\|$ is the Euclidean or 2-norm of $(\bullet)$, defined for an $N \times N$ matrix $\mathbf{C}$ as $\|\mathbf{C}\| \equiv \sqrt{\sum_{j=1}^{N} \sum_{i=1}^{N} |C_{ij}|^2}$. If the identified damping matrix and the one used in simulation match exactly then $N_{\text{abs}} = 0$. However this is rarely the case and a good indication of numerical matching between the measured and the identified damping matrix is when N_{abs} is very close to zero. On a logarithmic scale this would mean that a large negative value of $\log_{10}(N_{\text{abs}})$. Except where stated otherwise, all the norms will be plotted on a *negative logarithmic* scale. Hence a positive value in the plots should be considered as an indication of good performance of a given identification method.

The diagonal terms of the modal damping matrix are related to the natural frequencies and damping factors while the off-diagonal terms represent the coupling of undamped modes by damping [17]. A *modal norm* based on the diagonal part of the identified damping matrix in modal coordinates quantifies the extent to which the damping factors of each mode are fitted:

$$N_{\text{modal}} \equiv \left| \frac{\|\text{diag}(\mathbf{C}'_f) - \text{diag}(\mathbf{C}')\|}{\|\text{diag}(\mathbf{C}')\|} \right|, \tag{29}$$

where $\text{diag}(\mathbf{C}'_f)$, $\text{diag}(\mathbf{C}')$ are matrices containing the diagonal elements of the identified and exact damping matrices in modal coordinates.

An important but less studied feature of damping identification concerns the spatial distribution of damping in a vibrating system. To understand how well each of the identification methods fits the spatial distribution, a third norm based on the spatial patterns of the identified and original damping matrix is proposed. It indicates whether the identified damping matrix has the same qualitative spatial distribution as the one used in simulation. The *spatial* norm is defined as

$$N_{\text{spatial}} \equiv \left| \frac{\|\mathbf{C}_f^f - \mathbf{C}^f\|}{\|\mathbf{C}^f\|} \right|, \tag{30}$$

where $\mathbf{C}_f^f$ and $\mathbf{C}^f$ are the spatial *forms* of the fitted and the exact damping matrices in physical coordinates. These matrices are chosen to represent the spatial distribution independent of the magnitudes of damping. To illustrate this, consider the system shown in Fig. 1. It can be seen that the dampers couple the motion of the first and second masses but the motion of the third and fourth masses is not coupled by damping. Hence, in physical coordinates the damping matrix has non-zero terms on all diagonal elements of the damping matrix. However, the off-diagonal elements are non-zero only for the first two masses. To represent this pattern, the form of the damping matrix $\mathbf{C}^f$ is defined as

$$\mathbf{C}^f = \begin{bmatrix} 1 & -1 & 0 & 0 \\ -1 & 1 & 0 & 0 \\ 0 & 0 & 1 & 0 \\ 0 & 0 & 0 & 1 \end{bmatrix}. \tag{31}$$

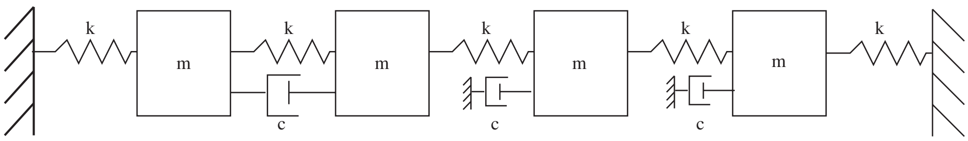

Fig. 1. A 4 dof non-proportionally damped system used in the simulation study of examples 1 and 2. The parameters are: $m = 1\,\text{kg}$, $k = 1\,\text{N/m}$, while $c = 0.02\,\text{Ns/m}$ for example 1 and $c = 0.2\,\text{Ns/m}$ for example 2.

Finally, an obvious way to check the accuracy of the identified damping matrix is to synthesise the FRFs by using the identified damping matrix, and compare them with the measured ones. This provides the basis for the fourth norm, the *reconstruction norm*, given by

$$N_{\text{recon}} \equiv \left\| \frac{|H_r(\omega)| - |H(\omega)|}{|H(\omega)|} \right\|, \tag{32}$$

where H and H_r are the original and the reconstructed FRFs, respectively.

6. Simulation examples

The choice of the simulation examples is motivated by the need to reproduce key features of typical vibration measurements. These are: random noise, modal incompleteness, i.e. a limited number of modes being used for vibration analysis, and spatial incompleteness, i.e. a small number of measurement points leading to inadequate spatial sampling of vibration modes of a continuous structure. The relative influence of these factors on the success of any given identification method is not entirely obvious. A systematic study involving test systems with increasing level of complexity is required.

Four idealised systems are chosen to test the damping identification methods. All of them are based on two simple discrete spring–mass–dashpot vibrating systems shown in Figs. 1 and 2.

Example 1 is a 4 dof system of discrete masses and springs with non-proportional viscous damping and low modal overlap of typically 0.01. The parameter values used in the simulation are as labelled in Fig. 1. The modes are almost real (imaginary parts very small compared to the real parts) due to the low modal overlap [17]. The modal overlap factor (μ_n) is the ratio of modal bandwidth to modal spacing given by $\mu_n \equiv \zeta_n\omega_n/(\omega_n - \omega_{n-1})$ where ω_n and ζ_n denote the nth natural frequency and damping factor, respectively. This system is complete in the sense that a 4×4 FRF matrix is used with no spatial or modal truncation. Since the modal overlap is low the modes are well separated. Thus modal fitting errors are expected to be small. Random noise in the "measured" FRFs is the main source of error in this example. The method of adding noise will be described shortly.

Example 2 is basically the same system as in example 1, but with much higher damping so that the modal overlap is of the order of 0.1. The increase in modal overlap results in modes with significant imaginary part [17]. It also means that the modes are closely spaced and hence more difficult to fit by modal fitting methods. This system is still complete. Thus, the sensitivity of identification methods in this case is due to modal fitting errors as well as noise.

Example 3 is a 10 dof system, shown in Fig. 2, with low modal overlap of typically 0.001. In this example, only the first four modes are retained for damping identification, i.e. modal truncation is made. However there is no spatial truncation since the FRFs are measured at all 10 dofs. This example reflects a measurement situation wherein only the well-excited modes are retained for modal identification and comparison purposes. Hence the "measurements" are *incomplete* in the modal domain. The sensitivity in this case is due to modal truncation and noise.

Example 4 is essentially the same system as that considered in example 3, but spatial truncation is brought into consideration in addition to modal truncation. The first four modes are retained and the "measurements" are assumed to be made on the 1st, 4th, 7th, and 10th masses only. Essentially, a 10 dof system with 10 modes is truncated to a 4 dof system with 4 modes in this example. Hence, the measurements are *incomplete* in the modal as well as the physical domains. This example can be considered as a representative test case corresponding to a measurement situation wherein the measurements are made over a grid of points and only

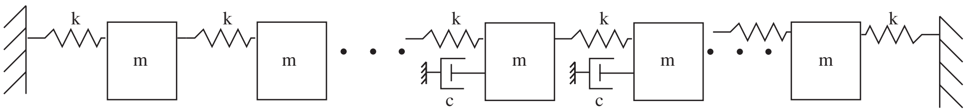

Fig. 2. A 10 dof system with viscous non-proportional damping used in examples 3 and 4. The dashpots are attached to masses 4 and 5. $m = 1\,\text{kg}$, $k = 4 \times 10^7\,\text{N/m}$, $c = 27\,\text{Ns/m}$.

well excited modes are retained for modal analysis. The sensitivity in this case is due to modal/spatial truncation and random noise. Because of low modal overlap the modal fitting errors are expected to be small.

A typical drive point FRF for each of the above simulation examples is shown in Fig. 3. Note that examples 3 and 4 are based on the same system.

7. Simulation procedure

The simulation study can be divided into four stages. In the first stage the dynamic stiffness matrix is constructed from the mass, stiffness and damping matrices which are known a priori. The FRF matrix is then obtained by inverting the dynamic stiffness matrix at every frequency point. The FRF matrix is obtained at 1024 frequency points covering a sufficient range of frequencies to include all natural frequencies.

The second stage of simulation involves adding random noise to the simulated FRFs to mimic the experiments. Gaussian random noise is generated using the MATLAB^{TM} random noise generator ("RANDN" function). At every frequency point the noisy FRF matrix is generated using the equation:

$$\mathbf{H}_{\text{noisy}}(\omega) = \mathbf{H}(\omega) + \frac{N_l}{100} 10^{(N_f/20)} \mathbf{N}, \tag{33}$$

where $\mathbf{N}$ is the matrix of random numbers, chosen from a normal distribution with zero mean, unit variance and standard deviation. N_l is the percentage noise level and N_f is a floor value which is chosen typically 5 dB below the peak response of the most highly damped mode in the frequency range considered. This model is, of course, only one among several possible noise models. For each noise case, 100 different realisations of the random number matrix are obtained, which are then used to ascertain the variability of the identified damping matrix obtained by using the same identification method.

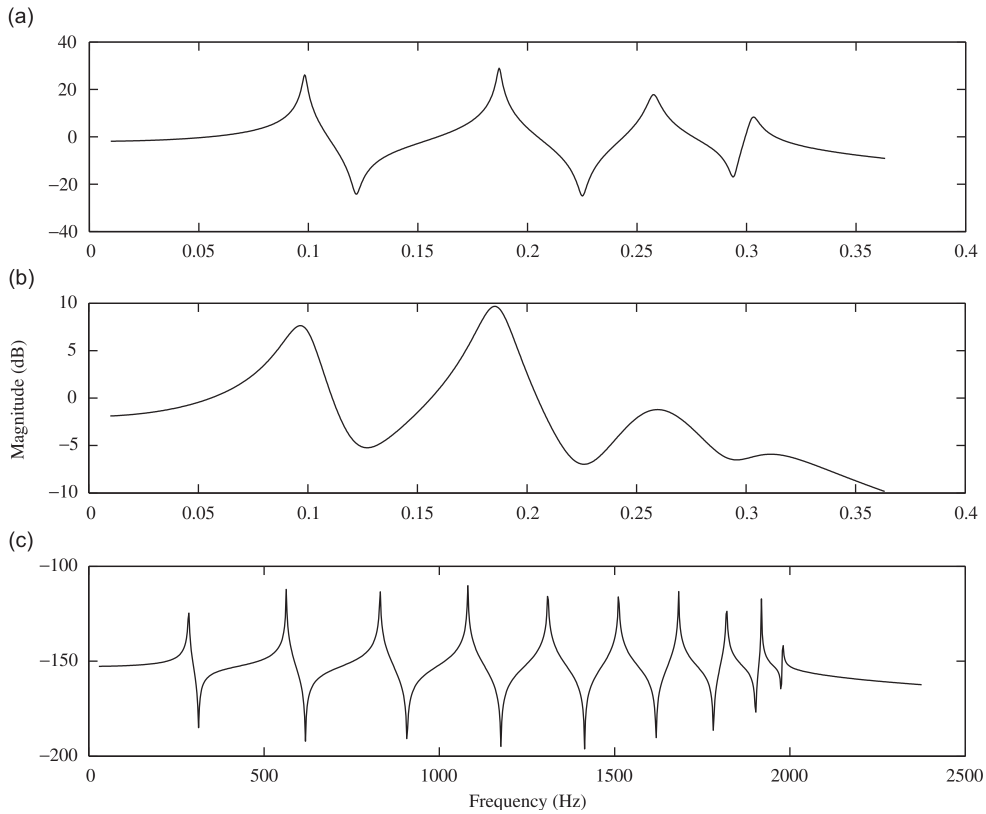

Fig. 3. Typical drive point FRFs of the four simulation examples. (a) system of example 1; (b) system of example 2; (c) system of examples 3 and 4.

The third stage is to identify the damping matrix using the algorithms discussed earlier. The fourth and final stage is to post-process the damping identification results and to compute the four measures of performance as detailed in Section 5.

8. Example 1: low modal overlap

The first example to be considered is the 4 dof system with light damping and consequently low modal overlap of typically 0.01. This example serves to illustrate the noise sensitivity of different methods. Other factors, such as modal identification errors and truncation errors have no significant influence.

Before presenting the results, it is necessary to consider the amount of data involved. There are 21 damping identification methods, and each method is tested for 4 noise levels. For each noise level in turn, 100 realisations are used to ascertain the variability of the identified damping matrix. Thus for each noise case one has to compare 2100 identified damping matrices and for 4 noise levels there are 8400 damping matrices. With this much information it is clearly not possible to present the full details of all the identified damping matrices for comparison purposes. Instead, the four measures of performance described in Section 5 will be shown for each identification method and noise case. Even so, the amount of information contained in each plot to be shown is very high. This inevitably means that some effort is needed for a complete understanding of these plots.

8.1. Typical identification results

It is helpful for orientation to discuss the norms of a representative set of methods in some detail. The identification methods chosen for this purpose are: Adhikari's viscous damping method based on complex modes and Lee and Kim's method based on the dynamic stiffness matrix. For Lee and Kim's method, three additional enhanced methods are also considered. The results for these five methods are shown in Fig. 4. Recall that the norms are plotted on a negative logarithmic ($-\log_{10}$) scale to cover a wide range of the numerical values. Positive values of the norm indicate good performance.

Consider first the absolute norm shown in Fig. 4(a). The mean and standard deviation (represented as an errorbar) over 100 noise realisations are shown together in the same plot. It can be seen that with increase in the noise level the numerical accuracy of the damping matrix identified by Adhikari's method progressively diminishes. However, this loss of accuracy is more pronounced for Lee and Kim's method. In fact, the negative value of the norm at 15% noise level indicates that the identified damping matrix is severely inaccurate. Enhanced methods, which are meant to improve the performance of the matrix methods such as Lee and Kim's method, show varying levels of success. Recall that enhanced methods simply change the FRF matrix input to the matrix methods. Positive improvements are achieved at higher noise levels with FRF expansion, i.e. synthesising the full FRF matrix from the modal parameters of one row or column of the FRF. This can be seen by the positive value of the norm, at high noise levels of 15%. It may also be noticed that at low levels of noise FRF expansion is less beneficial compared to the original matrix method. In strong contrast to this, FRF reconstruction does not help improve the performance. The enhanced method based on SVD gives comparable performance to the original matrix method at low noise levels but it completely fails at high noise levels.

The spatial norm in Fig. 4(b) shows a broadly similar pattern to that of the absolute norm in Fig. 4(a). It can be seen that whenever a damping matrix is identified which is good with respect to the absolute norm, the identified spatial distribution is also accurate.

Fig. 4(c) shows the modal norm which quantifies the matching between the modal damping factors calculated using the identified damping matrix and the actual values used in the simulation. In Adhikari's method the diagonal part of the modal damping matrix is obtained directly from modal fitting of FRFs, it is not surprising that this method "performs" well at all noise levels according to this norm. Contrast this with the absolute norm which shows a progressive loss of accuracy with the noise level. Lee and Kim's method on the other hand shows a very similar pattern to that already discussed for the absolute norm.

One important question is whether this sensitivity of the identified damping matrix has any influence on the degree of matching between the original and reconstructed FRFs. The reconstruction norm shown in Fig. 4(d)

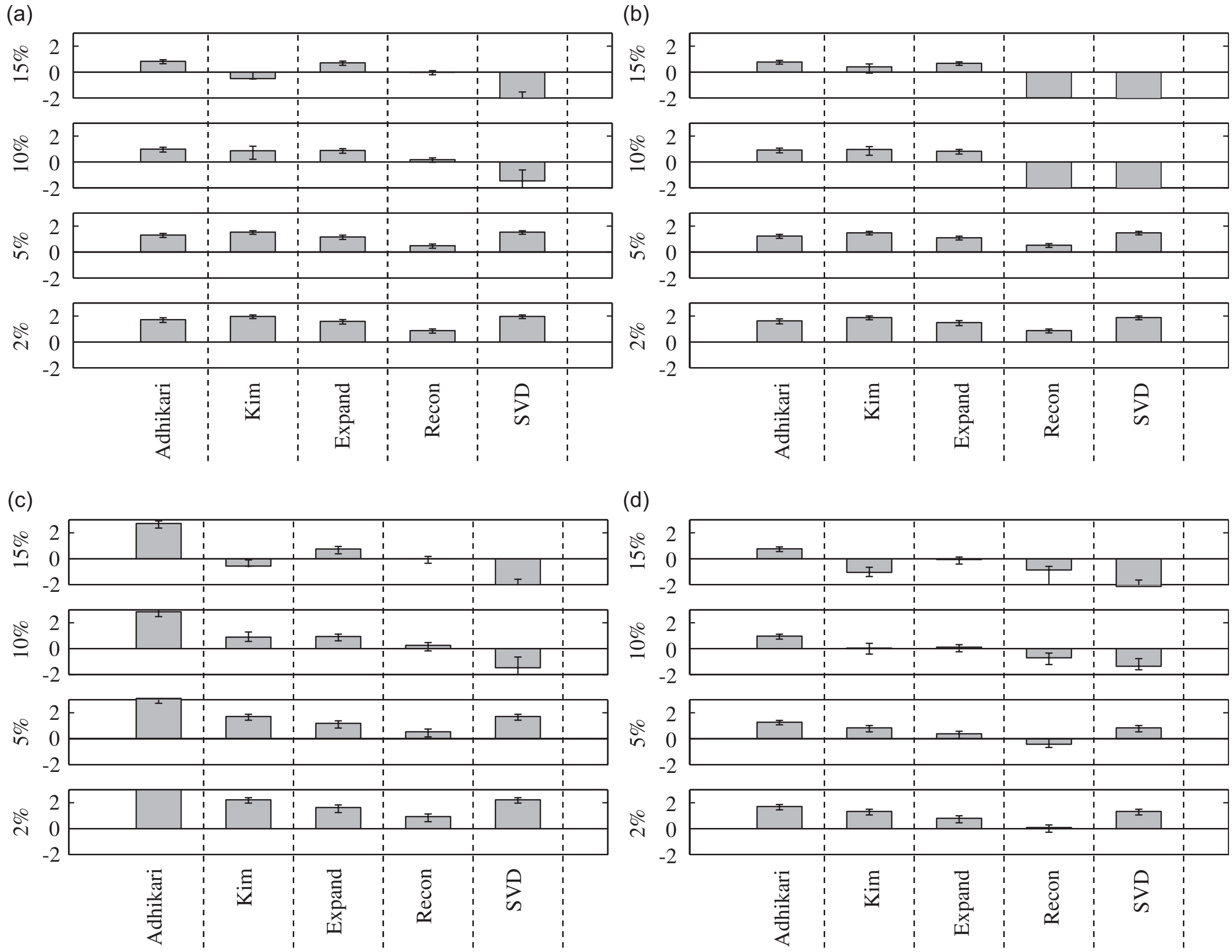

Fig. 4. Comparison of the performance of representative identification methods with respect to various norms. The mean and standard deviation (represented as error bar) over 100 noise realisations are shown together in the same plot. The norms are plotted in negative logarithmic scale and for the sake of comparison convenience the y-axis is limited to the chosen numerical range of 10^{-2}–10^{2}. Norms exceeding this range are truncated. The y-axis labels indicate the % noise levels in the FRFs used for identification. (a) Absolute norm; (b) spatial norm; (c) model norm; (d) reconstruction norm.

clearly shows that the sensitivity of the identified damping matrix does affect the reconstruction. The sensitivity exhibited by Adhikari's viscous method with respect to this norm is quite similar to the other three norms. The same can be said about Lee and Kim's method.

To illustrate the data used in computing this norm Fig. 5(a) shows the comparison between the actual (noise-free) and synthesised FRFs, for Adhikari's viscous damping identification method, for a particular noise realisation of two representative noise levels. As expected from the reconstruction norm in shown in Fig. 4(d) this method performs well. The reconstruction norm also suggests that Lee and Kim's method is poor at 15% noise level. This can be easily seen by observing the reconstructed FRFs for the first two modes, for example in Fig. 5(b). As the noise level increases the difference between the fitted and the original FRF becomes increasingly large. Thus it can be concluded, based on the absolute and the reconstruction norms, that Lee and Kim's method is very sensitive to high noise levels in this example.

The damping identification results will now be presented in the form of the four norms for all methods tested.

The absolute norm which quantifies the numerical matching between the identified and original damping matrices is shown in Fig. 6(a). The two methods of Adhikari, namely the viscous damping identification

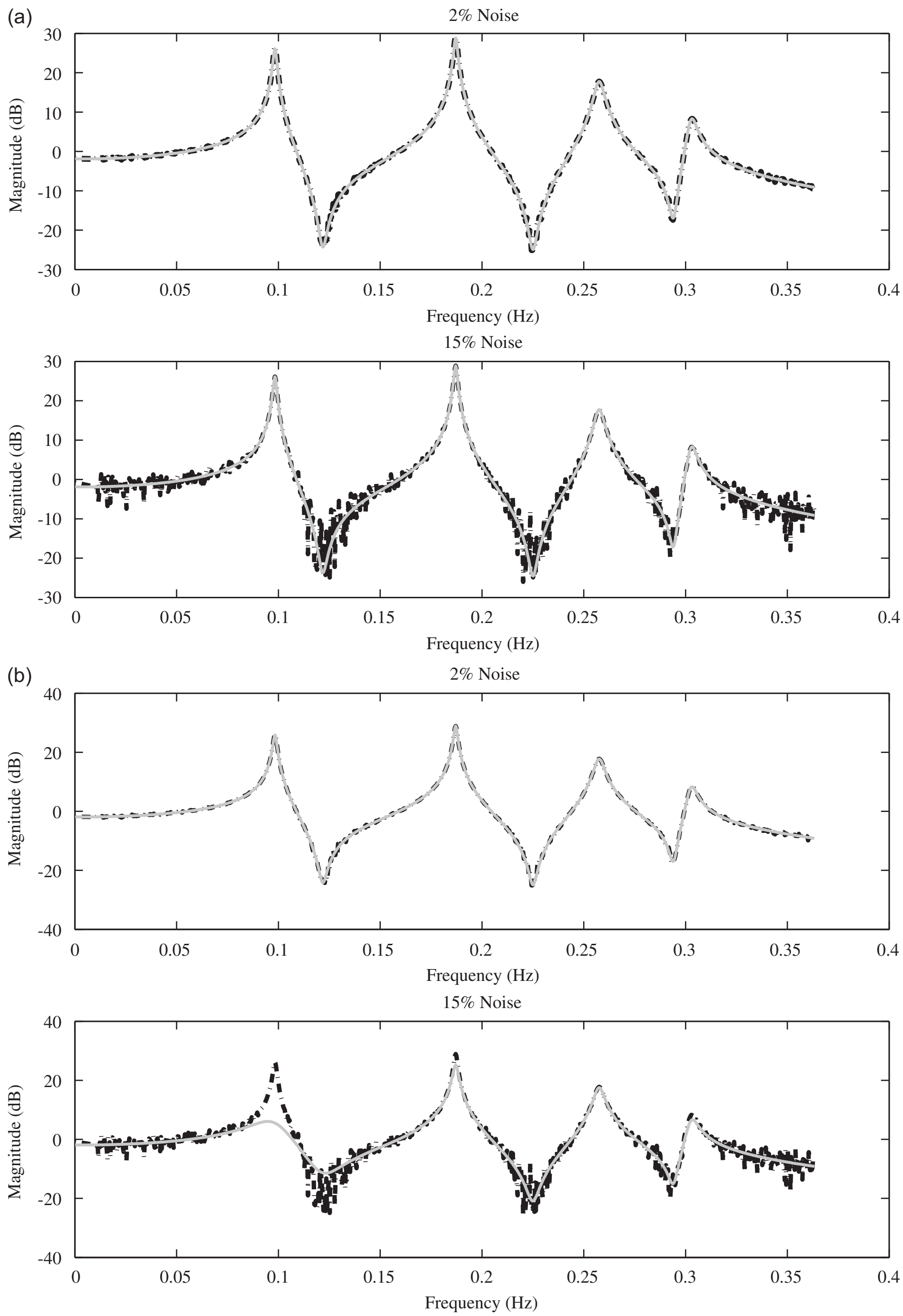

Fig. 5. Comparison of original and synthesised FRF $H_{11}(\omega)$: the dark dashed line represents the true FRF, the light solid line represents the fitted FRF. (a) Adhikari's viscous damping fitting method; (b) Kim's method.

method and a symmetric variant of the same, gradually lose their accuracy with increasing noise (compare the height of bars for each noise level for any given norm). This can be attributed to the modal fitting errors. Of the two methods, the symmetric viscous fitting method shows a slightly better performance. Similar sensitivity to noise is exhibited by other modal methods such as Lancaster's, Minas' and Ibrahim's methods, although

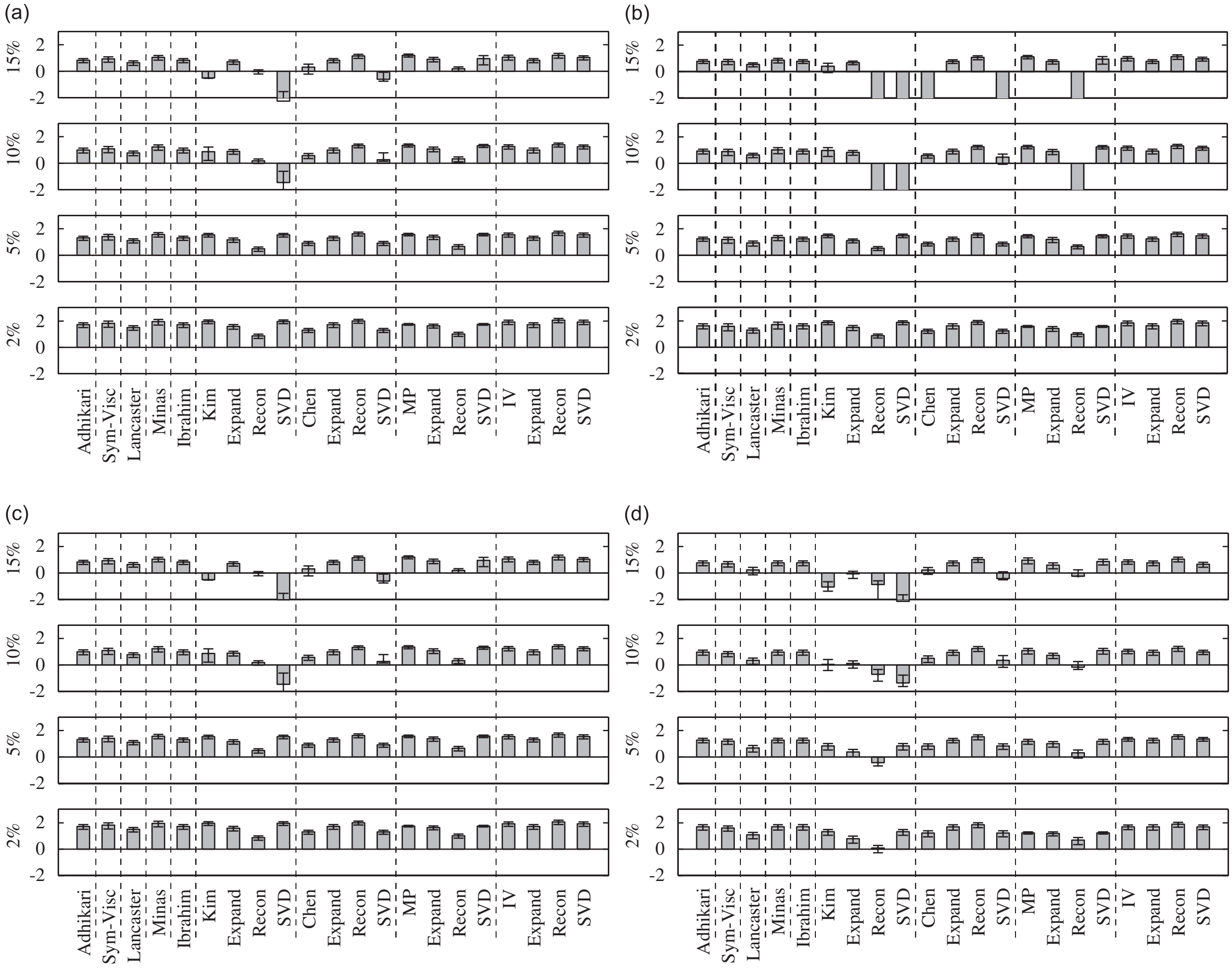

Fig. 6. Norms for example 1: system with low modal overlap. The mean and standard deviation (represented as error bar) over 100 noise realisations are shown together in the same plot. The norms are plotted in negative logarithmic scale and for the sake of comparison convenience the y-axis is limited to the chosen numerical range of 10^{-2}–10^{2}. The y-axis labels indicate the % noise levels in the FRFs used for identification. (a) Absolute norm; (b) spatial norm; (c) modal norm; (d) reconstruction norm.

Lancaster's method performs consistently less well than others in this test case. Among the matrix methods, Lee and Kim's method turns to out to be the most sensitive one, while the matrix perturbation and instrumental variable methods are more robust to noise.

The unusual sensitivity of Lee and Kim's method can be explained as follows. In this method, the damping matrix is fitted to the imaginary part of the dynamic stiffness matrix obtained by inverting the FRF matrix. In the presence of noise, the imaginary part of the dynamic stiffness matrix gets "mixed up" with the real part. This contamination of the imaginary part of the dynamic stiffness matrix increases with the noise level. Thus at higher noise levels, the contribution to the imaginary part of the dynamic stiffness matrix comes not only from the damping matrix but also from the mass and stiffness matrices. Hence the sensitivity of this identification method.

Enhanced methods are expected to cope better with the noise and hence improve the performance of the original matrix methods. In these methods, the original noisy FRFs are replaced with much cleaner ones. These cleaned up FRFs can be generated by reconstructing the FRFs, expanding the full FRF matrix from the modal parameters of the first row of the FRF matrix or by applying the SVD technique. The improvement of any given matrix method by the enhanced methods is highly dependent on the information that they need from measurements, and on whether enhanced methods can help provide better information than the raw measurements in this regard. As can be seen from Fig. 6(a), FRF reconstruction and expansion do help improve the performance of Chen's method. However in the case of Lee and Kim's method only FRF expansion helps. Enhanced methods based on FRF reconstruction do not improve the performance at all and in some cases make it worse. This may be due to the fact that the imaginary part of the dynamic stiffness synthesised using the enhanced methods may not be accurate.

To investigate this possibility, the norm of the imaginary part of the dynamic stiffness matrix synthesised using the three enhanced methods is computed for different noise levels and shown in Fig. 7. The true value, computed from the exact matrices known in simulations, is also shown. It can be seen that only the FRF expansion method reproduces the correct imaginary part of the dynamic stiffness matrix. For the enhanced method based on the FRF reconstruction large deviations from the true value are produced near the resonance peaks in the FRFs (see Fig. 7(b)). Since the FRFs created by the enhanced method are not so accurate with regard to the imaginary part of the dynamic stiffness matrix, Lee and Kim's method did not perform well. For the SVD method the norm of the imaginary part of the dynamic stiffness matrix is very noisy and hence the errors in the damping matrix identified therefrom. Thus the particular details of a matrix method govern the usefulness of a particular enhanced method. Since Lee and Kim's method requires accurate information on the imaginary part of the dynamic stiffness matrix, of the three enhanced methods only the FRF expansion technique helps improve the performance of the original matrix method.

One of the chief advantages with the enhanced methods based on the FRF expansion is that the number of measurements are reduced, i.e. one need not measure the FRF for all excitation/measurement locations. Given this data reduction, the enhanced methods based on FRF expansion are certainly an improvement over their corresponding matrix methods. The enhanced methods based on FRF reconstruction are found to help Chen's and the IV method while Lee and Kim's and the matrix perturbation method do not benefit at all. SVD based enhanced methods seem to be the least effective of the three in improving the performance of the matrix methods.

The spatial norm quantifies the extent to which the identified damping matrix reproduces the spatial distribution of energy dissipation sources within the vibrating system. The pattern of the spatial norm shown in Fig. 6(b) is similar to that of the absolute norm shown in Fig. 6(a). Hence the discussion made in the absolute norm case is also applicable to this norm. The modal norm is based on the diagonal elements of the modal damping matrix and it is a measure of how well the damping factors of each mode are fitted. The modal norm shown in Fig. 6(c) also shows similar patterns to that of absolute norm in Fig. 6(b).

The reconstruction norm is based on comparing two FRFs, namely, the FRFs reconstructed using the fitted damping matrix (and mass and stiffness matrices), and the FRF obtained by inverting the exact dynamic stiffness matrix. One would expect the "measured" FRFs and reconstructed FRFs to match better if the natural frequencies and modal damping factors are fitted well by the identified damping matrix. Since the modal norm quantifies the accuracy of modal damping fitting, there is a direct correlation between reconstruction and modal norms which can be seen by comparing Figs. 6(c) and (d). Whenever the spatial norm and modal norm indicate poor performance the same is reflected in the reconstruction norm.

9. Example 2: moderate modal overlap

This simulation example is based on essentially the same system as that considered in example 1, except that the dashpot coefficients are now increased by a factor of 10. This increase in damping adds additional features to the data, some of which are beneficial and some are not:

(1) Increase in the modal overlap increases the imaginary part of modes [17], which is beneficial to modal methods.
(2) Modal fitting errors may become significant due to higher modal overlap, which has a detrimental effect on modal and enhanced methods based on FRF reconstruction and FRF expansion.
(3) Matrix methods based on the dynamic stiffness matrix are expected to benefit due to the increased damping, because the imaginary part of the dynamic stiffness matrix is no longer small compared to the real part and hence is less affected by noise.

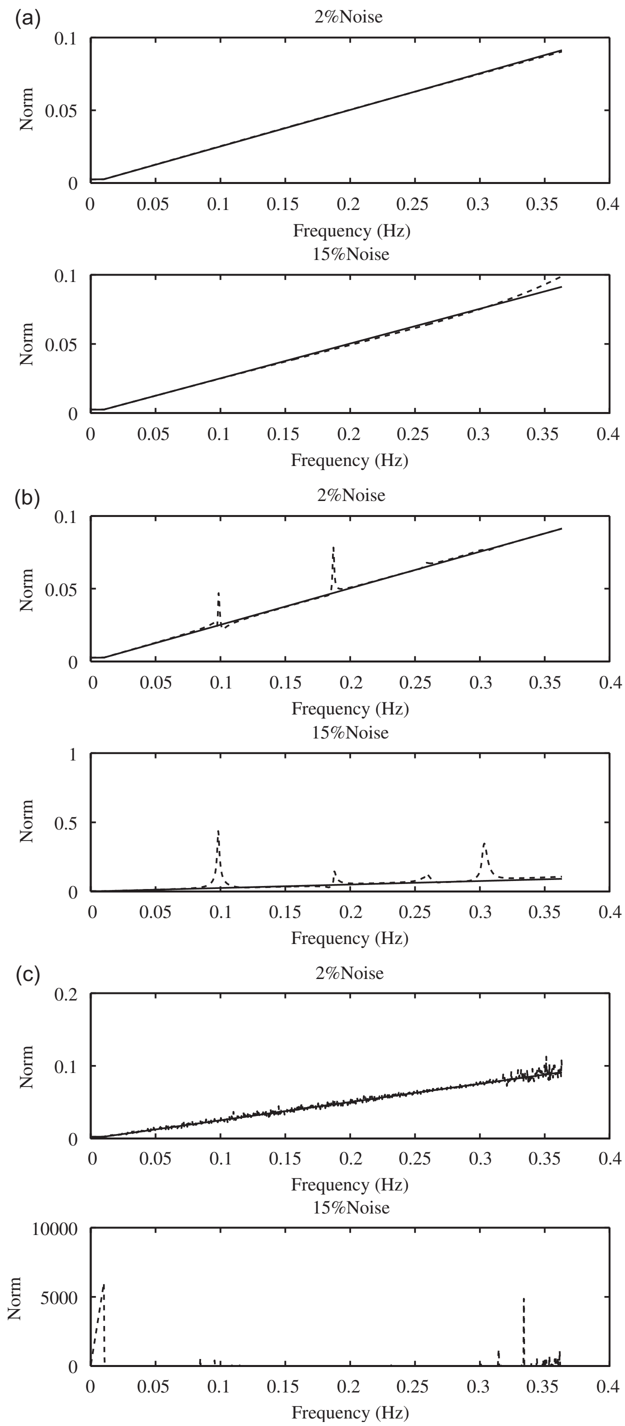

Fig. 7. Comparison of errors in the imaginary part of the dynamic stiffness matrix for the three enhanced methods. The *y*-axis is the norm of the imaginary part of the dynamic stiffness matrix: the solid line represents the true value and the dashed line is obtained using the FRF synthesised by the respective enhanced methods. (a) Expansion; (b) reconstruction; (c) SVD.

(4) Since the damping matrix is of comparable magnitude to both the stiffness and mass matrices (about 10% of the stiffness matrix in this example), the assumption of small damping may not be valid. This is expected to affect matrix methods which are based on the small damping assumption, in particular the matrix perturbation method.

Fig. 8(a) shows the absolute norm for various identification methods and noise levels. Except Lancaster's method, all the modal methods seem to show good performance with respect to this norm. Based on this norm, one may be tempted to conclude that the modal parameter estimation errors are not very important. However, the final judgement on the success of an identification method should be based on the reconstruction norm to be discussed shortly.

The matrix methods, especially Lee and Kim's method which was very sensitive in the low modal overlap example (see Fig. 6(a) for comparison), turned out to be more robust to noise in this example. This marked improvement can be explained by point (3) above. The matrix perturbation method which is based on the small damping assumption is not so good compared to other matrix methods. This can be attributed to the fact that the small damping assumption will be less accurate for this example. The enhanced methods give comparable performance to the original matrix methods.

The spatial norm in Fig. 8(b) reveals a broadly similar sensitivity to that of the absolute norm. Except Lancaster's method, all methods perform well with respect to modal norm shown in Fig. 8(c). The reconstruction norm is the norm with respect to which the judgement on the success of an identification method could be made. It is shown in Fig. 8(d) for various damping identification methods. In contrast to the modal methods, the reconstruction norm for all matrix methods indicates good performance.

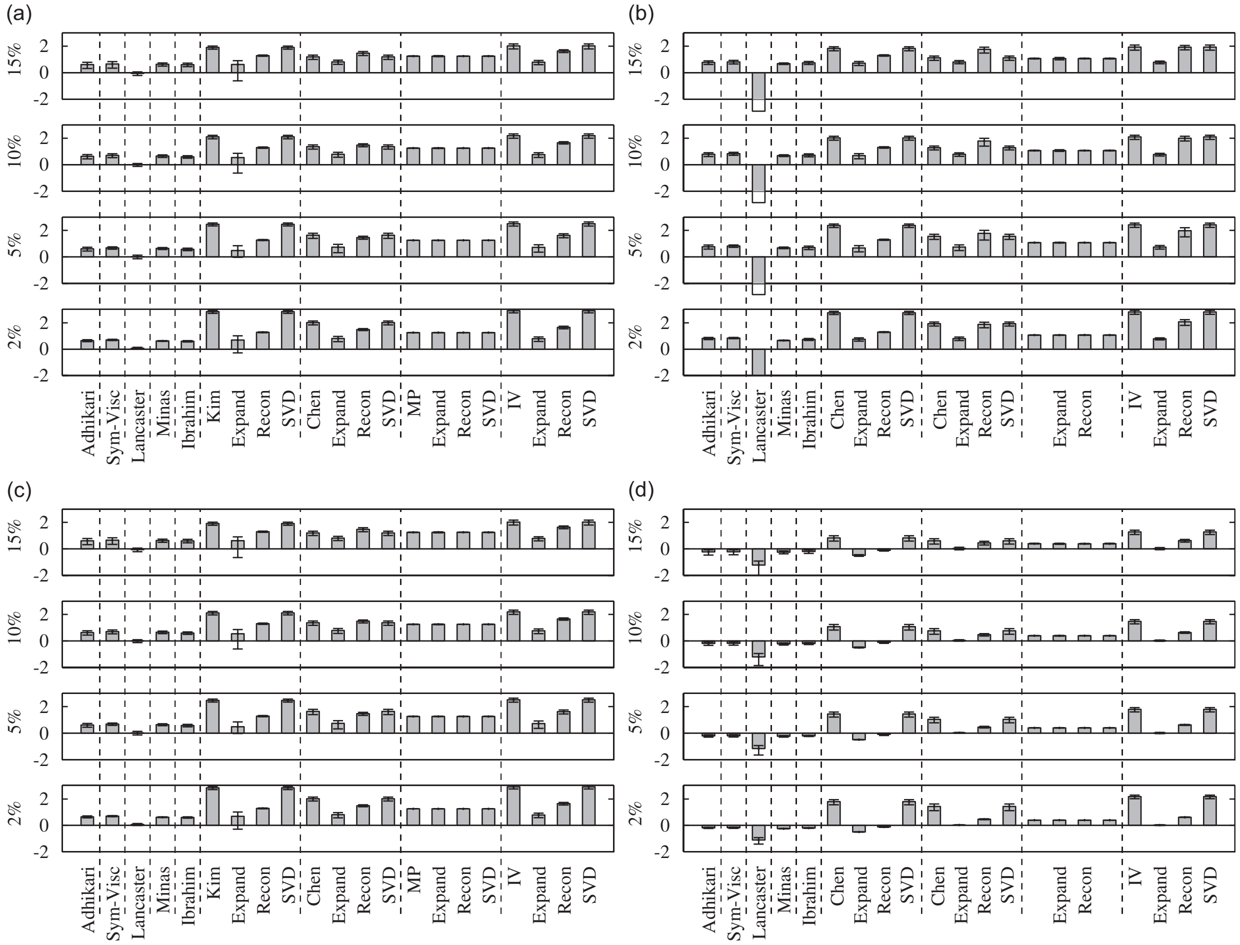

Fig. 8. Norms for example 2: system with high modal overlap. The mean and standard deviation (represented as error bar) over 100 noise realisations are shown together in the same plot. The norms are plotted in negative logarithmic scale and for the sake of comparison convenience the y-axis is limited to the chosen numerical range of 10^{-2}–10^{2}. The y-axis labels indicate the % noise levels in the FRFs used for identification. (a) Absolute norm; (b) spatial norm; (c) modal norm; (d) reconstruction norm.

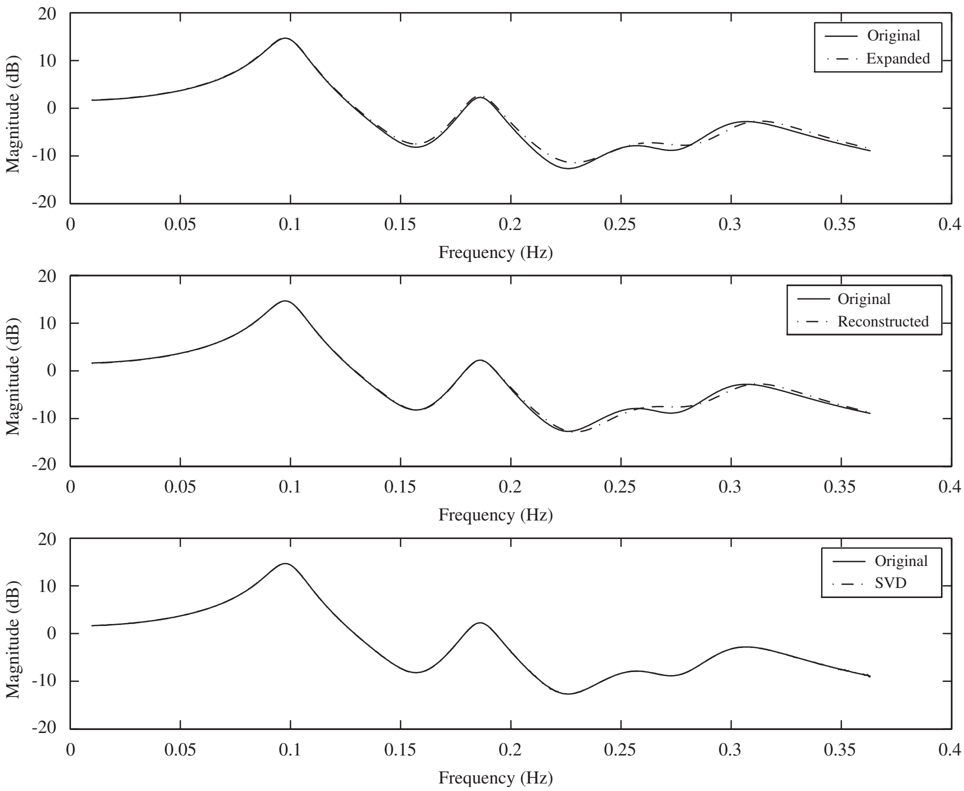

Fig. 9. Comparison of FRFs for example 2 for 2% noise case: FRFs synthesised by enhanced methods and noise-free FRFs.

Among the matrix methods, the matrix perturbation method seems to be the least accurate. This can be due to two reasons: the modal fitting errors due to increased modal overlap will reduce the accuracy of the diagonal part of the modal damping matrix, and the series expansion for the FRF may require additional terms.

All enhanced methods except the one based on expansion of FRFs give comparable performance. Modal fitting errors are the main source for the reduced accuracy of FRF expansion. The sensitivity of the enhanced methods can be better understood by comparing the FRF matrix which is input to matrix methods with the noise free FRF matrix. Fig. 9 shows typical FRFs obtained by the three enhanced methods for 2% noise case. It can be observed that enhanced methods based on FRF expansion and reconstruction fail to reproduce the original FRF due to the failure of modal fitting methods. Given that the FRF matrix input to the matrix methods is not accurate, the matrix methods are not improved by the enhanced methods. This is reflected in the reconstruction norm in Fig. 8(d).

10. Example 3: modal incompleteness

One important feature of vibration data which has not been studied in the previous examples is that of incompleteness. In practice, it is inevitable that vibration test data is incomplete from a modal point of view since an infinite number of modes of vibration cannot be excited, measured and analysed. Similarly it is not possible to measure modes at all points on the test structure: modes are sampled at the chosen grid of points. This brings in another feature of experimental data, namely that of spatial incompleteness. Discussion of these aspects of measurement is given in Ref. [8].

The current example deals with modal incompleteness and the next example incorporates both spatial and modal incompleteness. A 10 dof viscously damped system (shown in Fig. 2) is simulated in both examples. In this example, only the first four modes, of the possible 10 modes, are used to identify the damping matrix.

The damping matrix with respect to which the identified damping matrix must be compared to compute the absolute norm is not immediately obvious for this example. Two damping matrices can be used: either the full damping matrix used in simulations, or a truncated damping matrix. The truncated damping matrix can be obtained by transforming the 10×10 damping matrix from physical to modal coordinates, truncating this to the first four modes and transforming back to the physical coordinates using the 4 retained modes sampled at all 10 dofs so that the truncated matrix in physical coordinates is still of size 10×10. Thus two absolute norms can be computed for this simulation example, based on either the original damping matrix used in simulation or the damping matrix corresponding to 4 modes retained in the modal coordinates. Both versions are shown in Figs. 10(a) and (b).

One important feature to note from these figures is that Adhikari's methods and the matrix perturbation method change from being poor with respect to the absolute norm computed using the full damping matrix to being very good with respect to the absolute norm computed using the truncated damping matrix. This is primarily due to modal truncation involved with modal methods and the matrix perturbation method. The opposite effect can be observed for the matrix methods: IV method, Lee and Kim, and Chen's methods.

One might expect that the matrix methods should not be affected by modal truncation since they fit the damping matrix using the dynamic stiffness matrix. Hence it is possible to fit the full damping matrix by matrix methods, despite the fact that the FRF matrix is truncated to include only the first few modes. In this regard, only the IV method seems to perform well. Among the modal methods, symmetric viscous fitting is better compared to the unsymmetrised one while all other modal methods perform poorly. This is true with respect to both the absolute norms. Among the matrix methods the matrix perturbation seems to be very robust to noise sensitivity compared to other methods. The other matrix methods such as Lee and Kim's method and Chen's method perform poorly with respect to both the absolute norms even at low noise level. The IV method, however, performs well only at low noise and becomes very poor even at moderate noise levels.

Similar to the absolute norms, two spatial norms based on the full and truncated damping matrix can be computed. They are as shown in Figs. 10(c) and (d). The strong correlation between these figures and their corresponding figures in the case of the absolute norm suggests that the discussion pertaining to the absolute norm is relevant to this norm as well.

The results for the modal norm are shown in Fig. 10(e). The results shown in this figure are quite contrasting to the absolute and spatial norms discussed earlier. It is clear from this figure that, even though the identified damping matrix does not reproduce the spatial pattern accurately, nor is numerically close to the truncated and full damping matrices, nevertheless the modal damping factors of retained modes are fitted well. This can be confirmed by comparing the absolute, the spatial and the modal norms for various identification methods. In this regard, the norms for the IV method and the matrix perturbation method can be cited as good examples. This suggests that in order to fit the individual damping factors of each mode, the accuracy of the damping matrix in physical coordinates does not matter very much. Alternatively, several damping matrices in physical coordinates can lead to the same diagonal terms of the modal damping matrix. This issue will be further examined in the next example involving both modal and spatial truncation.

With respect to the modal norm, all modal methods perform equally well and have similar noise sensitivity. Among the matrix methods Lee and Kim's method is the most sensitive while the matrix perturbation method is the least. In general, enhanced methods help improve the performance of the corresponding matrix methods. The reconstruction norm based on comparing the reconstructed and original FRFs is shown in Fig. 10(f). Strong correlation between the modal and reconstruction norms can be immediately noticed by comparing Figs. 10(e) and (f).

The best methods among modal methods are: Adhikari's (both), Lancaster's, and Ibrahim's methods while the method proposed by Minas and Inman seems to be very poor. Among the matrix methods, the matrix perturbation method is the most robust to noise sensitivity whereas the other methods progressively deteriorate. Most enhanced methods do not help improve the performance of matrix methods in this example.

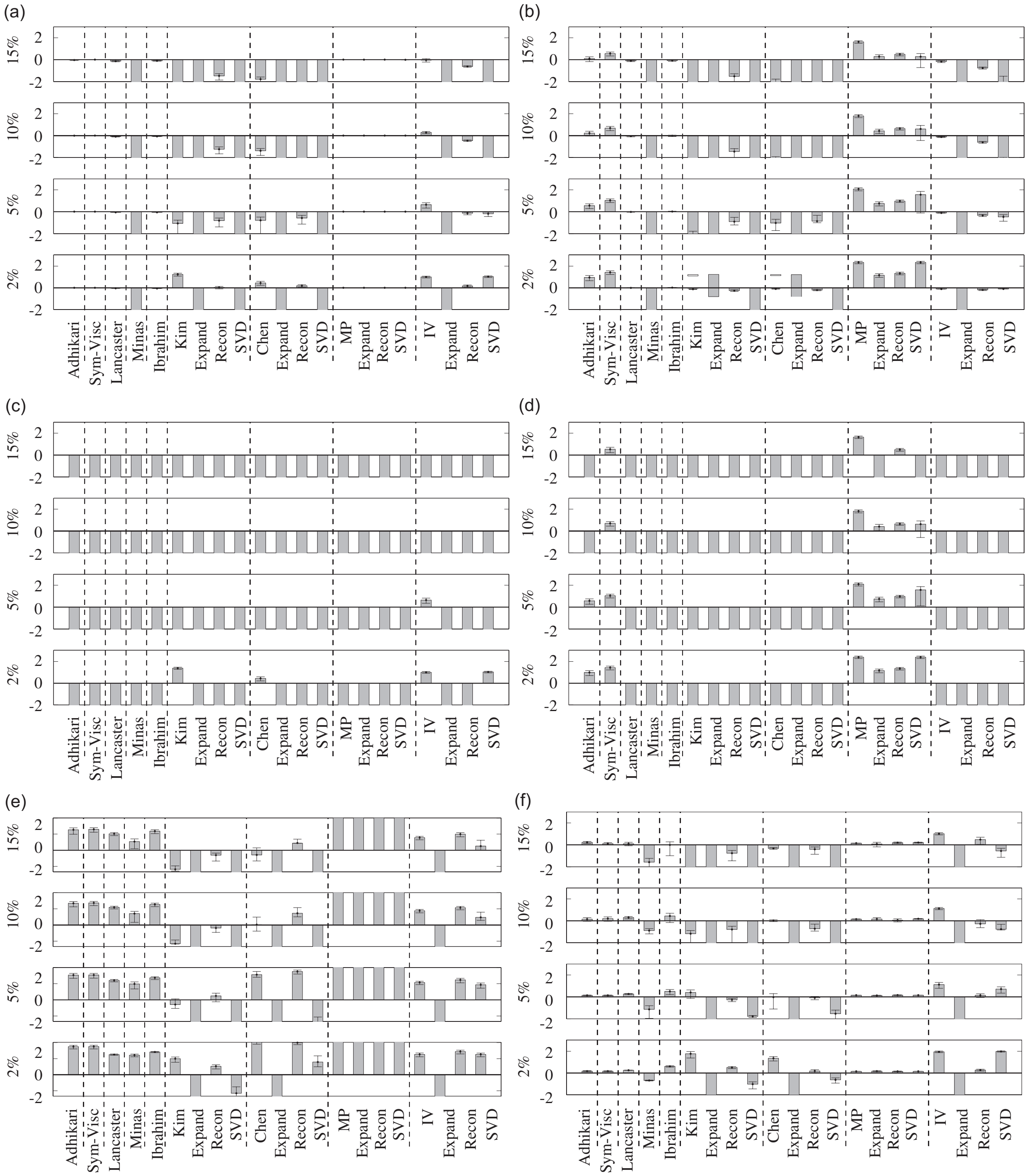

Fig. 10. Norms for example 3: a 10 dof system truncated to the first 4 modes in the frequency domain. The mean and standard deviation (represented as error bar) over 100 noise realisations are shown together in the same plot. The norms are plotted in negative logarithmic scale and for the sake of comparison convenience the *y*-axis is limited to the chosen numerical range of 10^{-2}–10^{2}. The *y*-axis labels indicate the % noise levels in the FRFs used for identification. The absolute and spatial norms are computed based on the full damping matrix for norms labelled as 1 and truncated damping matrix for norms labelled as 2. (a) Absolute norml; (b) absolute norm2; (c) spatial norm1; (d) spatial norm2; (e) modal norm; (f) reconstruction norm.

11. Example 4: modal and spatial truncation

The final simulation example incorporates both modal and spatial incompleteness of FRF data. The first 4 modes of vibration are assumed to be measured at dofs 1, 4, 7 and 10. Due to the truncation of modes and spatial sampling, the mass, stiffness and damping matrices have to be reduced to the size of the reduced system. In this case the reduced system is of size 4×4 since the response of the system is sampled at only 4 dofs. The reduced mass, stiffness and damping matrices are obtained using the iterated IRS method [26]. The reduced system matrices are:

$$\mathbf{M} = \begin{bmatrix} 3.5471 & 0.3510 & -0.5538 & 0.6937 \\ 0.3510 & 2.5512 & 0.4911 & -0.5538 \\ -0.5538 & 0.4911 & 2.5512 & 0.3510 \\ 0.6937 & -0.5538 & 0.3510 & 3.5471 \end{bmatrix}, \tag{34a}$$

$$\mathbf{K} = 10^7 \begin{bmatrix} 8.8867 & -2.1705 & -0.7771 & 1.7772 \\ -2.1705 & 3.1280 & -1.2622 & -0.7771 \\ -0.7771 & -1.2622 & 3.1280 & -2.1705 \\ 1.7772 & -0.7771 & -2.1705 & 8.8867 \end{bmatrix}, \tag{34b}$$

$$\mathbf{C} = \begin{bmatrix} 4.5551 & -9.7503 & -4.7744 & 3.3783 \\ -9.7503 & 47.8711 & 10.2198 & -7.2315 \\ -4.7744 & 10.2198 & 5.0043 & -3.5410 \\ 3.3783 & -7.2315 & -3.5410 & 2.5056 \end{bmatrix}. \tag{34c}$$

A natural question concerning the reduced systems is whether the spatial distribution of damping of the complete system is still preserved. Unfortunately, the general answer to this question is still elusive given the computational manipulations involved in model reduction techniques. However, for the particular system studied, it can be observed that the spatial distribution of damping is very roughly preserved. In the original complete system the dampers are attached to masses 4 and 5 whereas in the reduced system damping appears to be concentrated around the second mass, which corresponds to the 4th mass of the complete system.

With these reduced system matrices, the norms are computed to compare the performance of the damping identification methods.

The absolute norm is shown in Fig. 11(a), for all the damping identification methods. Among the modal methods Adhikari's symmetrised method and Ibrahim's method seem to be the best methods while all other methods perform poorly. Among the matrix methods the matrix perturbation method and the instrumental variable methods are very robust. The other two matrix methods are poor. Enhanced methods based on FRF expansion and reconstruction fail to improve the robustness of original matrix methods.

The spatial norm which quantifies whether or not the fitted damping matrices reproduce the correct spatial distribution is shown in Fig. 11(b). Here, the form of the spatial distribution is obtained using Eq. (34c). It can be seen that apart from the IV method all other matrix identification methods fail to reproduce the correct spatial pattern of the damping. Enhanced methods are of no avail with respect to this norm.

The modal norm, calculated based on the diagonal elements of the truncated modal damping matrix, is shown in Fig. 11(c). The most striking feature exhibited by all the identification methods is that, despite being unable to reproduce an accurate damping matrix or the correct spatial pattern, the diagonal part of the modal damping matrix is still accurate. This is the case for more than one identification method, which suggests that even if the identified damping matrix does not well represent the spatial distribution of dissipation sources within a structure, one can still expect to fit modal damping factors accurately. The reverse is also true, i.e. by mere modal fitting of a set of modes of a vibrating system, one may not expect to fit the spatial distribution of underlying damping mechanisms. Note that this was also the case with example 3 which had modal truncation only.

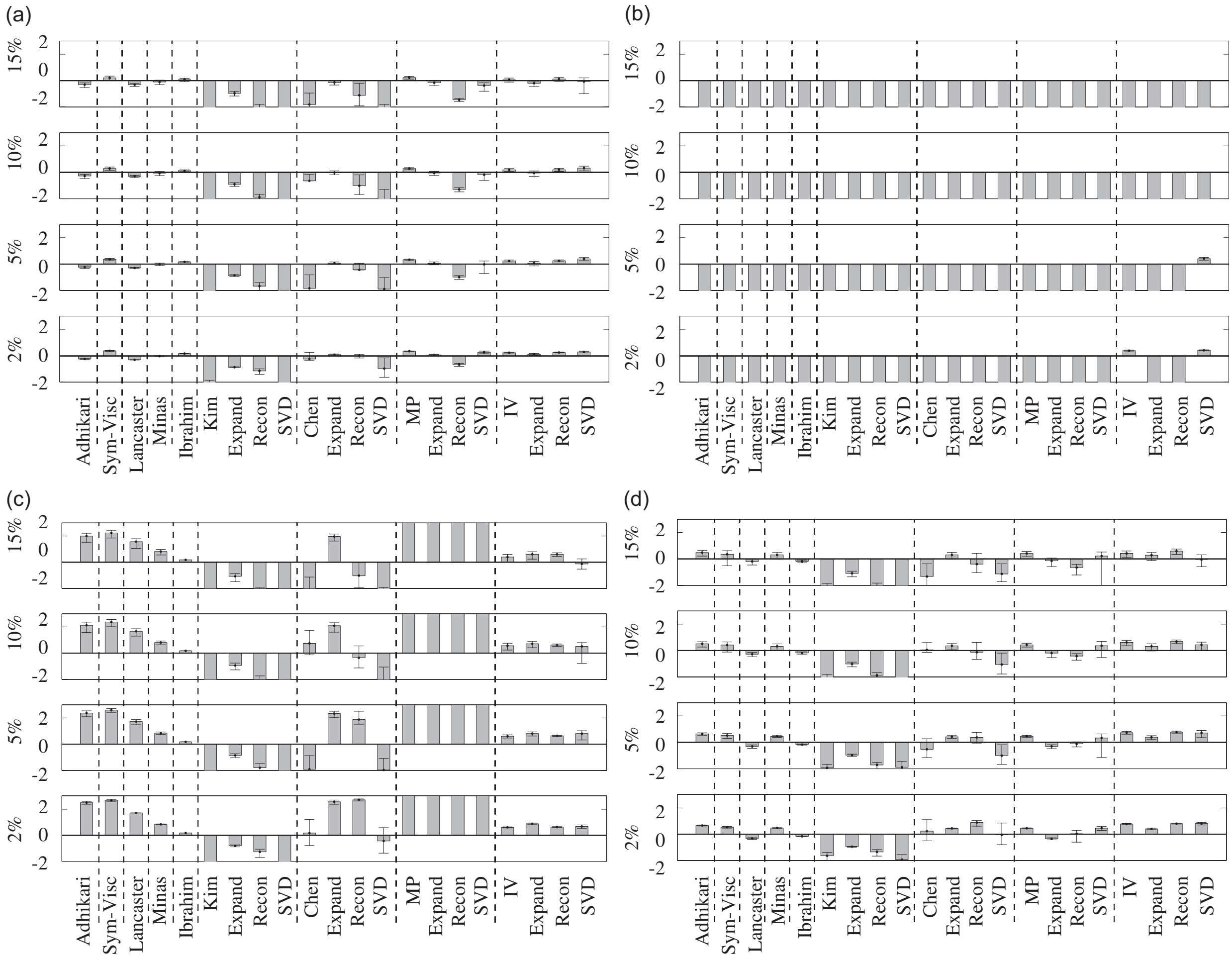

Fig. 11. Norms for example 4: a 10 dof non-proportionally damped system truncated to 4 modes and 4 dofs. The mean and standard deviation (represented as error bar) over 100 noise realisations are shown together in the same plot. The norms are plotted in negative logarithmic scale and for the sake of comparison convenience the y-axis is limited to the chosen numerical range of 10^{-2}–10^{2}. The y-axis labels indicate the % noise levels in the FRFs used for identification. (a) Absolute norm; (b) spatial norm; (c) modal norm; (d) reconstruction norm.

Table 1
Summary of damping identification methods

Group	Method	Input	Output	Remarks
Modal parameter methods	Viscous	$\mathbf{\Psi}, \mathbf{\Lambda}, \mathbf{M}$	$\mathbf{C}$	
	Symmetrised-viscous	$\mathbf{\Psi}, \mathbf{\Lambda}, \mathbf{M}$	$\mathbf{C}$	
	Lancaster	$\mathbf{\Psi}, \mathbf{\Lambda}, \mathbf{M}, \mathbf{C}_o$	$\mathbf{C}$	
	Minas and Inman	$\mathbf{\Psi}, \mathbf{\Lambda}, \mathbf{M}, \mathbf{K}$	$\mathbf{C}$	
	Ibrahim	$\mathbf{\Psi}, \mathbf{\Lambda}, \mathbf{M}, \mathbf{K}$	$\mathbf{C}$	
Matrix methods	Lee and Kim	$\mathbf{H}$	$\mathbf{M}, \mathbf{C}, \mathbf{K}$	
	Chen, Ju and Tesui	$\mathbf{H}$	$\mathbf{M}, \mathbf{C}, \mathbf{K}$	
	Instrumental variable method	$\mathbf{H}$	$\mathbf{M}, \mathbf{C}, \mathbf{K}$	
	Matrix perturbation	$\mathbf{H}$, $\mathbf{M}$, $\mathbf{C}_o$	$\mathbf{C}$	**New**
Enhanced methods	Expansion	$\mathbf{H}$ (one row)	$\mathbf{H}$ (full matrix)	**New**
	Reconstruction	$\mathbf{H}$ (noisy)	$\mathbf{H}$ (reconstructed)	**New**
	SVD	$\mathbf{H}$ (noisy)	$\mathbf{H}$ (SVD)	**New**

Table 2
Overall summary of damping identification methods: ✓ indicates good performance and × indicates poor performance

Method	Noise sensitivity	Truncation	Modal overlap	Computing cost	Analytical model required
Viscous	✓	✓	×	Low	
Symmetrised-viscous	✓	✓	✓	Low	
Lancaster	✓	×	×	High	
Minas and Inman	✓	✓	×	High	Yes
Ibrahim	✓	✓	×	High	Yes
Lee and Kim	×	×	✓	Moderate	
Expansion	×	×	×	Moderate	
Reconstruction	×	×	×	Moderate	
SVD	×	×	✓	Moderate	
Chen et al.	✓	✓	✓	Moderate	
Expansion	✓	✓	×	Moderate	
Reconstruction	✓	✓	×	Moderate	
SVD	×	×	×	Moderate	
Matrix perturbation	✓	✓	✓	Moderate	
Expansion	✓	×	×	Moderate	
Reconstruction	✓	✓	✓	Moderate	
SVD	✓	✓	✓	Moderate	
IV method	✓	✓	✓	Moderate	
Expansion	✓	×	×	Moderate	
Reconstruction	✓	✓	✓	Moderate	
SVD	✓	✓	✓	Moderate	

As one might expect, accurate identification of the decay rate and natural frequency of each mode will automatically lead to a better FRF reconstruction. This can be verified by comparing the modal norm in Fig. 11(c) and the reconstruction norm in Fig. 11(d).

12. Conclusions

The damping identification methods summarised in Tables 1 and 2 have been systematically studied via four simulation examples and classified as being good or poor according to their performance with regard to the four norms. The following main conclusions emerge from the simulation study presented here:

(1) Among the modal methods Adhikari's symmetrised viscous fit is the best method: it can cope well with both noise and truncation errors.
(2) Among the matrix methods, the matrix perturbation method (new method proposed in this paper), the instrumental variable (IV) method, and Chen's method are the best algorithms to fit the damping matrix. Lee and Kim's method is well suited for systems with high damping but very poor for systems with low damping.
(3) The performance of enhanced methods is mixed in the simulation examples studied. In general, the FRF expansion and reconstruction techniques help Chen's method at high noise levels but fail to improve the performance of Lee and Kim's method. The matrix perturbation and IV methods do not benefit from the enhanced method. The enhanced method based on SVD gives comparable performance to the original matrix methods at low noise levels but fails to help at high noise levels.
(4) An important finding of the simulation study is that even though the spatial distribution of damping is not well represented, the FRFs may be well reconstructed. This suggests that spatial distribution of damping is the most sensitive aspect of the identification and hence cannot be relied upon.

Acknowledgement

The authors would like to acknowledge the financial support, during the course of this work, through the award of a Cambridge Nehru fellowship from Cambridge Commonwealth Trust, UK; Nehru Trust for

Cambridge University, New Delhi, India. Bursaries from St. John's College, University of Cambridge, are thankfully acknowledged.

References

[1] L. Gaul, The influence of damping on waves and vibrations, *Mechanical Systems and Signal Processing* 13 (1) (1999) 1–30.
[2] E.E. Ungar, The status of engineering knowledge concerning the damping of built-up structures, *Journal of Sound and Vibration* 26 (1) (1973) 141–154.
[3] C.W. Bert, Material damping: an introductory review of mathematical models, measures and experimental techniques, *Journal of Sound and Vibration* 29 (2) (1973) 129–153.
[4] S.H. Crandall, The role of damping in vibration theory, *Journal of Sound and Vibration* 11 (1) (1970) 3–18.
[5] W. Weaver, P. Jonhston, *Structural Dynamics by Finite Elements*, first ed., Prentice-Hall, Englewood Cliffs, NJ, 1987.
[6] A. Srikantha Phani, Damping Identification in Linear Vibrations, PhD Thesis, Cambridge University Engineering Department, Cambridge, January 2004.
[7] D.J. Ewins, *Modal Testing*, second ed., Research Studies Press Ltd., Taunton, Somerset, UK, 2000.
[8] N.M. Maia, J. Silva (Eds.), *Theoretical and Experimental Modal Analysis*, first ed., Research Studies Press Ltd., Taunton, Somerset, UK, 2000.
[9] J.H. Lee, J. Kim, Identification of damping matrices form measured frequency response functions, *Journal of Sound and Vibration* 240 (3) (2001) 545–565.
[10] S.Y. Chen, M.S. Ju, Y.G. Tsuei, Estimation of mass, stiffness and damping matrices form frequency response functions, *Journal of Vibration and Acoustics, ASME* 118 (1996) 78–82.
[11] C.-P. Fritzen, Identification of mass, and stiffness matrices of mechanical systems, *Journal of Vibration and Acoustics, ASME* 108 (1986) 9–16.
[12] S. Adhikari, J. Woodhouse, Identification of damping—part 1: viscous damping, *Journal of Sound and Vibration* 219 (5) (1999) 43–61.
[13] S. Adhikari, J. Woodhouse, Identification of damping—part 2: non-viscous damping, *Journal of Sound and Vibration* 219 (5) (1999) 63–88.
[14] P. Lancaster, Free vibration and hysteretic damping, *Journal of the Royal Aeronautical Society* 64 (1960) 229.
[15] C. Minas, D.J. Inman, Identification of a nonproportional damping matrix from incomplete modal information, *Journal of Vibration and Acoustics, ASME* 113 (1990) 219–224.
[16] S.R. Ibrahim, Dynamic modelling of structures from measured complex modes, *AIAA Journal* 21 (6) (1983) 898–901.
[17] J. Woodhouse, Linear damping models for structural vibration, *Journal of Sound and Vibration* 215 (3) (1998) 547–569.
[18] J.W. Rayleigh, *The Theory of Sound*, vol. 1, Dover, New York, 1894 reprint 1945.
[19] A. Bhaskar, Damping in Mechanical Vibrations: New Methods of Analysis and Estimation, PhD Thesis, Cambridge University Engineering Department, 1992.
[20] A. Bhaskar, Estimates of errors in the frequency response of non-classically damped systems, *Journal of Sound and Vibration* 184 (1) (1995) 59–72.
[21] R.A. Horn, C.R. Johnson, *Matrix Analysis*, Cambridge University Press, Cambridge, 1985.
[22] S. Adhikari, Damping Models for Structural Vibration, PhD Thesis, Cambridge University Engineering Department, 2000.
[23] D.F. Pilkey, D.J. Inman, An iterative approach to viscous damping matrix identification, *International Modal Analysis Conference* (*IMAC*), 1997, pp. 1152–1157.
[24] W.H. Press, S.A. Teukolsky, W.T. Vetterling, B.P. Flannery, *Numerical Recipes in C*, second ed., Cambridge University Press, Cambridge, 1992.
[25] A. Thite, D.J. Thompson, The quantification of structure-borne transmission paths by inverse methods—part 1: improved singular value rejection methods, *Journal of Sound and Vibration* 264 (2003) 411–431.
[26] M.I. Friswell, S.D. Garvey, J.E.T. Penny, Model reduction using dynamic and iterated IRS techniques, *Journal of Sound and Vibration* 186 (2) (1995) 311–323.